

COSTAS G. VAYENAS  
COSTAS PLIANGOS  
SUSANNE BROSDA  
DIMITRIOS TSIPLAKIDES

Department of Chemical  
Engineering University of Patras,  
Patras, Greece

REVIEW PAPER

66.087+541.128:681.516.52

## RULES AND MODELING OF PROMOTION, ELECTROCHEMICAL PROMOTION AND METAL-SUPPORT INTERACTIONS

*During the last three years there have been some interesting developments in catalysis and solid state electrochemistry. First the functional identity has been shown of Promotion, Electrochemical Promotion (NEMCA effect) and metal-support interactions. Second, the concept of absolute potential has been defined in solid state electrochemistry together with its intimate relationship to the work function of catalytic supports and thus to metal-support interactions. Third rigorous rules have been established for promotion, electrochemical promotion and metal-support interactions. These rules enable one to predict the type of promoter or support needed to promote any catalytic reaction on the basis of its unpromoted kinetics. Fourth, a rigorous extension of Langmuir-Hinshelwood kinetics has been developed which accounts explicitly for the interaction of adsorbates with the double layer formed at the catalyst/gas interface. This new type of catalytic kinetic is excellent qualitative agreement with experiment.*

*These new concepts are summarized and discussed here with emphasis to the recent discovery that promotion, electrochemical promotion and metal-support interactions are catalysis in presence of an electrochemical double layer.*

### 1. INTRODUCTION

Promotion [1,2] of catalyst nanoparticles, electrochemical promotion (NEMCA) of porous and of single crystal catalyst films [2,3] and metal nanoparticle-support interactions [2] are three, at a first glance, independent phenomena which can all dramatically affect catalytic activity and selectivity on metal and metal oxide catalyst surfaces.

Recent experimental and theoretical work has shown that the three phenomena are intimately related via the action of spillover to the point that one may conclude that the three phenomena are functionally identical and only operationally different [2].

In this communication we review some of the key phenomenological aspects of promotion, electrochemical promotion and metal-support interactions, underline their kinetic similarities and common fundamental origin on the basis of surface spectroscopic and theoretical investigations, including the new concept of the absolute potential of supports [2] and discuss some key experiments which prove their identical nature, i.e. catalysis in presence of a controllable double layer at the catalyst/gas interface.

We then discuss the recently [2] established rules of promotion and electrochemical promotion and an extension of Langmuir-Hinshelwood kinetics, based on an effective medium double layer isotherm model, which is in good qualitative agreement with experiment and allows one to make predictions about the effect of promoters, but also of catalyst supports, on the kinetics of different catalytic reactions.

#### 1.1. Basic principles and terminology

##### 1.1.1. Promotion

The term *promotion*, or classical promotion, is used to denote the action of a substance, called

*promoter*, which when added to a catalyst, usually on its surface, enhances its catalytic performance, i.e. it increases the rate of a catalytic reaction or the selectivity to a desired product, or the useful lifetime of the catalyst.

For example K or K<sub>2</sub>O is a promoter of Fe for the synthesis of ammonia or for the production of higher hydrocarbons in the Fischer-Tropsch synthesis.

Broadly speaking promoters can be divided into *structural promoters* and *electronic promoters*. In the former case they enhance and stabilize the dispersion of the nanoparticle-dispersed active phase on the catalyst support. In the latter case they enhance the catalytic properties of the active phase itself. This stems from their ability to modify the chemisorptive properties of the catalyst surface and to significantly affect the chemisorptive bond strength of reactants and intermediates. At the molecular level this is the result of direct ("through the vacuum") and indirect ("through the metal") interactions. The term "through the vacuum" denotes direct electrostatic, Stark type, attractive or repulsive, interactions between the adsorbed reactants and the local electric field created by the coadsorbed promoter. The term "through the metal interaction" refers to changes in the binding state of adsorbed reactants due to promoter-induced redistribution of electrons near the Fermi level of the metal [1,2].

Denoting by  $\theta_P$  the coverage of a promoter on a catalyst surface and by  $p_j$  the partial pressures of the reactants,  $j$ , of the catalytic reaction which is being promoted, we can formulate mathematically the above definition of a promoter as:

$$\left(\frac{\partial r}{\partial \theta_P}\right)_P > 0 \Leftrightarrow P \text{ is a promoter} \quad (1)$$
$$\left(\frac{\partial r}{\partial \theta_P}\right)_P < 0 \Leftrightarrow P \text{ is a poison}$$

The promotional propensity of a promoter,  $P$ , can be quantified by defining [2,3] a promotional index,  $Pl_P$ , from:

Author address: C.G. Vayenas, Department of Chemical Engineering, University of Patras, Caratheodory 1 St, GR-26500 Patras, Greece

Paper received and accepted: December 17, 2001

$$PI_P = (\Delta r/r_0)/\Delta\theta_P \quad (2)$$

where  $r_0$  is the unpromoted catalytic rate.

Thus the promotional index  $PI_P$  is positive for promoters and negative for poisons. In the latter case the definition of  $PI_P$  coincides with that of the "toxicity" defined by Barbier several years ago [4]. In the case of pure site blocking it is  $PI = -1$ . Values of  $PI_{O^{2-}}$  up to 150 and  $PI_{Na^{\delta+}}$  up to 6000 have been measured [2,3].

Another useful parameter for quantifying the promotional action is the promotional rate enhancement ratio,  $\rho_P$ , defined from:

$$\rho_P = r/r_0 \quad (3)$$

Promotional rate enhancement ratios,  $\rho_P$ , values of the order 10–100 are rather common [1,2] as we shall also see in this paper.

A promoter is not, in general, consumed during a catalytic reaction. Many millions of catalytic turnovers usually take place on a promoted site of a classically promoted catalyst before the promoter gets deactivated. The ratio of the promoter average lifetime on the catalyst surface,  $\tau_{PR}$ , over that of the catalytic reactants,  $\tau_R$ , is usually in excess of 10 [7]:

$$\tau_{PR}/\tau_R > 10^7 \Leftrightarrow \text{classical promotion} \quad (4)$$

When the promoter gets consumed at a faster rate, which is still, however, smaller than that of the catalytic reactant, then the promoter is termed *sacrificial promoter*. [2,3] This is the case, as we will see, in electrochemical promotion utilizing  $O^{2-}$  conducting solid electrolytes. The promoting  $O^{2-}$  species is introduced via a Faradaic process on the catalyst surface at a rate of  $I/2F$ , where  $I$  is the applied current and  $F$  is Faraday's constant. At steady state,  $I/2F$  also equals the rate of consumption of the sacrificial promoter  $O^{2-}$  species on the catalyst surface.

Using the standard definition [2, 3, 5–8] of the Faradaic efficiency,  $\Lambda$ , of an electrochemically promoted process:

$$\Lambda = \Delta r/(I/2F) \quad (5)$$

one can easily show that:

$$\tau_{PR}/\tau_R = \Lambda\rho_P/(\rho_P-1) \quad (6)$$

When  $\rho_P \gg 1$ , as is very frequently the case, Equation reduces to:

$$\tau_{PR}/\tau_R = \Lambda \quad (7)$$

which shows that the Faradaic efficiency,  $\Lambda$ , of electrochemically promoted reactions expresses the ratio of the average lifetimes of promoting species ( $O^{2-}$ ,  $Na^{\delta+}$ ) and of the key reactants on the catalyst surface [2,3].

Promoters are usually added to a catalyst during catalyst preparation (classical or chemical promotion). Thus if they get somehow lost (evaporation) or deactivated during prolonged catalyst operation, this leads to significant catalyst deterioration. Their

concentration cannot be controlled in situ, i.e. during catalyst operation. One of the most important advantages of electrochemical promotion is that it permits direct in situ control of the amount of the promoter on the catalyst surface.

### 1.1.2. Electrochemical promotion

Electrochemical promotion of catalysis (EPOC) or non-Faradaic electrochemical modification of catalytic activity (NEMCA) is the phenomenon whereby application of small current density ( $1-10^4 \mu A/cm^2$ ) or potential ( $\pm 2$  V) between a conductive catalyst, deposited on a solid electrolyte, and a second (catalytically inert) electrode, also deposited on the solid electrolyte, enhances the catalytic performance of the catalyst [2, 3, 5–18] (Fig. 1).

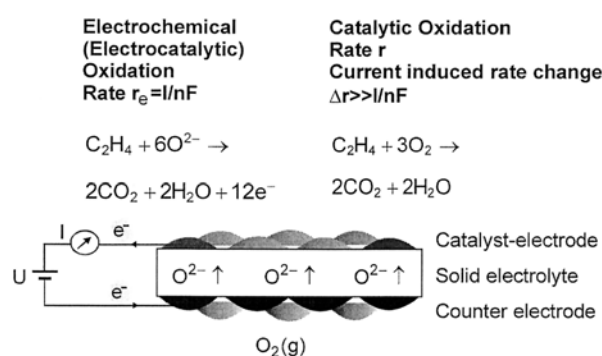


Figure 1. Experimental setup used in electrochemical promotion (NEMCA) experiments.

In electrochemical terms the catalyst also acts as the *working* electrode of the solid electrolyte cell which is formed, the second (catalytically inert) electrode is the *counter* electrode, while a third metal film, acting as a *reference* electrode is also useful to deposit on the solid electrolyte for fundamental EPOC studies. In this way one can study the dependence of the catalytic rate,  $r$ , on the catalyst-working electrode as a function of the potential difference,  $U_{WR}$ , between the catalyst-working (W) electrode and the reference (R) electrode (Fig. 1) [3,19–23].

The counter and the reference electrodes can be in a separate gaseous compartment (fuel cell type design) or can be in the same gaseous compartment with the catalyst-electrode (single chamber type design) [3,20–23].

The magnitude of electrochemical promotion can be quantified by the following three parameters:

(1) The Faradaic efficiency,  $\Lambda$ , already defined in Equation (5):

$$\Lambda = \Delta r/(I/2F) \quad (5)$$

where  $r$  is expressed in mol O, or more generally:

$$\Lambda = \Delta r/(I/F) \quad (8)$$

where  $r$  is expressed in g-equivalent.

A reaction is electrochemically promoted, or exhibits NEMCA, when  $|\Lambda| > 1$ . When  $\Lambda > 1$ , i.e. when the reaction rate is enhanced with positive current and increasing catalyst potential  $U_{WR}$ , the reaction is termed *electrophobic*. When  $\Lambda < -1$ , i.e. when the rate is enhanced with negative current and decreasing catalyst potential, the reaction is termed *electrophilic*.

Clearly the limits of electrocatalysis are  $|\Lambda| \leq 1$  [3]. Faradaic efficiency,  $\Lambda$ ,  $\nu$  values up to  $3 \times 10^5$  and down to

$-3 \cdot 10^4$  have been measured for different catalytic systems (Table 1) [3, 5, 6, 10–14, 16, 19, 21–79].

(2) The rate enhancement ratio,  $\rho$ , which, similar to the case of classical promotion (Eq. 3)), is defined from:

$$\rho = r/r_0 \quad (9)$$

As shown in Table 1,  $\rho$  values as high as 150 and as low as zero (complete catalyst poisoning) have been measured for different catalytic reactions.

Table 1. Electrochemical promotion studies classification based on the type of solid electrolyte

### 1. EP studies utilizing YSZ. Promoting ion: $O^{2-}$

Reactants		Products	Catalyst	T (°C)	$\Lambda_{max}(>0)$ or $\Lambda_{min}(<0)$	$\rho_{max}(>1)$ or $\rho_{min}(<1)$	$P _{O^{2-}}$	Ref.
Electron Donor (D)	Electron Acceptor (A)							
C <sub>2</sub> H <sub>4</sub>	O <sub>2</sub>	CO <sub>2</sub>	Pt	280–450	$3 \times 10^5$	55	55	6, 19, 24
C <sub>2</sub> H <sub>6</sub>	O <sub>2</sub>	CO <sub>2</sub>	Pt	270–500	300 –100	20 7	20 –	25
CH <sub>4</sub>	O <sub>2</sub>	CO <sub>2</sub>	Pt	600–750	5	70	70	3, 26
CO	O <sub>2</sub>	CO <sub>2</sub>	Pt	300–550	$2 \times 10^3$ –500	3 6	2 –	27
CO	O <sub>2</sub>	CO <sub>2</sub>	Pt	468–558	1000	5	5	3, 28, 29
CH <sub>3</sub> OH	O <sub>2</sub>	H <sub>2</sub> CO, CO <sub>2</sub>	Pt	300–500	$1 \times 10^4$	4, 15*	3	3, 30
C <sub>3</sub> H <sub>6</sub>	O <sub>2</sub>	CO <sub>2</sub>	Pt	350–480	$-3 \times 10^3$	6	–	31
CH <sub>3</sub> OH		H <sub>2</sub> CO, CO, CH <sub>4</sub>	Pt	400–500	–10	3*	–	22, 30
C <sub>2</sub> H <sub>4</sub>	NO	CO, CO <sub>2</sub> , N <sub>2</sub> , N <sub>2</sub> O	Pt	380–500	–50	7	–	32
C <sub>2</sub> H <sub>4</sub>	O <sub>2</sub>	CO <sub>2</sub>	Rh	250–400	$5 \times 10^4$	90	90	21, 23, 33
H <sub>2</sub>	CO <sub>2</sub>	CH <sub>4</sub> , CO	Rh	300–450	200	3*	2	3
C <sub>3</sub> H <sub>6</sub>	NO, O <sub>2</sub>	N <sub>2</sub> , N <sub>2</sub> O, CO <sub>2</sub>	Rh	250–450	$1 \times 10^3$	150*	15	34
CO	NO, O <sub>2</sub>	N <sub>2</sub> , N <sub>2</sub> O, CO <sub>2</sub>	Rh	250–450	20	20*	20	35
C <sub>2</sub> H <sub>4</sub>	O <sub>2</sub>	CO <sub>2</sub>	Pd	290–360	$10^4$	2	–	36, 37
CO	O <sub>2</sub>	CO <sub>2</sub>	Pd	400–550	$1 \times 10^3$	2	1	3, 22
H <sub>2</sub>	CO	C <sub>x</sub> H <sub>y</sub> , C <sub>x</sub> H <sub>y</sub> O <sub>z</sub>	Pd	300–370	10	3*	2	3
H <sub>2</sub> S		S <sub>x</sub> , H <sub>2</sub>	Pt	600–750	–	11	10	3, 38
CH <sub>4</sub>	O <sub>2</sub>	CO <sub>2</sub>	Pd	380–440	$2 \times 10^3$	90	90	36, 39
H <sub>2</sub>	CO <sub>2</sub>	CO	Pd	500–590	–50	10	–	3, 22
CO	NO	CO <sub>2</sub> , N <sub>2</sub> , N <sub>2</sub> O	Pd	320–480	–700	3	–	40, 41
CO	N <sub>2</sub> O	CO <sub>2</sub> , N <sub>2</sub>	Pd	440	–20	2	–	40
C <sub>2</sub> H <sub>4</sub>	O <sub>2</sub>	C <sub>2</sub> H <sub>4</sub> O, CO <sub>2</sub>	Ag	320–470	300	30*	30	5, 42–44
C <sub>3</sub> H <sub>6</sub>	O <sub>2</sub>	C <sub>3</sub> H <sub>6</sub> O, CO <sub>2</sub>	Ag	320–420	300	2*	1	3, 45
CH <sub>4</sub>	O <sub>2</sub>	CO <sub>2</sub> , C <sub>2</sub> H <sub>4</sub> , C <sub>2</sub> H <sub>6</sub>	Ag	650–850	5	30*	30	3, 46
CO	O <sub>2</sub>	CO <sub>2</sub>	Ag	350–450	20	15	15	3, 47
CH <sub>3</sub> OH		H <sub>2</sub> CO, CO, CH <sub>4</sub>	Ag	550–750	–25	6*	–	3, 48
CH <sub>3</sub> OH	O <sub>2</sub>	H <sub>2</sub> CO, CO <sub>2</sub>	Ag	500	–95	2	–	16
CH <sub>4</sub>	O <sub>2</sub>	C <sub>2</sub> H <sub>4</sub> , C <sub>2</sub> H <sub>6</sub> , CO <sub>2</sub>	Ag	700–750	–1.2	8*	–	49, 50
CO	O <sub>2</sub>	CO <sub>2</sub>	Ag–Pd	450–500	30	5	4	51
CH <sub>4</sub>	H <sub>2</sub> O	CO, CO <sub>2</sub>	Ni	600–900	12	2*	–	3, 52
CO	O <sub>2</sub>	CO <sub>2</sub>	Au	450–600	–60	3	–	49, 50
CH <sub>4</sub>	O <sub>2</sub>	CO <sub>2</sub>	Au	700–750	–3	3*	–	49, 50, 53
C <sub>2</sub> H <sub>4</sub>	O <sub>2</sub>	CO <sub>2</sub>	IrO <sub>2</sub>	350–400	200	6	5	11, 54
C <sub>2</sub> H <sub>4</sub>	O <sub>2</sub>	CO <sub>2</sub>	RuO <sub>2</sub>	240–500	$4 \times 10^3$	115	115	55

### 2. EP studies utilizing F<sup>–</sup> conductors

Reactants		Products	Catalyst	Solid Electrolyte	T (°C)	$\Lambda_{max}(>0)$ or $\Lambda_{min}(<0)$	$\rho_{max}(>1)$ or $\rho_{min}(<1)$	$P _{F^-}$	Ref.
Electron Donor (D)	Electron Acceptor (A)								
CO	O <sub>2</sub>	CO <sub>2</sub>	Pt	CaF <sub>2</sub>	500–700	200	2.5	1.5	3, 56

## 3. EP studies utilizing mixed conductors

Reactants		Products	Catalyst	Solid Electrolyte	T (°C)	$\Lambda_{\max(>0)}$ or $\Lambda_{\min(<0)}$	$\rho_{\max(>1)}$ or $\rho_{\min(<1)}$	$PI_{O_2}$	Ref.
Electron Donor (D)	Electron Acceptor (A)								
C <sub>2</sub> H <sub>4</sub>	O <sub>2</sub>	CO <sub>2</sub>	Pt	TiO <sub>2</sub> (TiO <sub>x</sub> <sup>+</sup> , O <sup>2-</sup> )	450–600	5x10 <sup>3</sup>	2	0	2
C <sub>2</sub> H <sub>4</sub>	O <sub>2</sub>	CO <sub>2</sub>	Pt	CeO <sub>2</sub> (CeO <sub>x</sub> <sup>+</sup> , O <sup>2-</sup> )	500	-10 <sup>5</sup>	3	-	58
C <sub>2</sub> H <sub>4</sub>	O <sub>2</sub>	CO <sub>2</sub>	Pt	YZTi10 <sup>#</sup>	400–475	-250	2	-	59
C <sub>3</sub> H <sub>6</sub>	O <sub>2</sub>	CO <sub>2</sub>	Pt	YZTi10 <sup>#</sup>	400–500	1000 -1000	2.4	-	59

4. EP studies utilizing Na<sup>+</sup> conductors

Reactants		Products	Catalyst	Solid Electrolyte	T (°C)	$\Lambda_{\max(>0)}$ or $\Lambda_{\min(<0)}$	$\rho_{\max(>1)}$ or $\rho_{\min(<1)}$	$PI_{Na^+}$	Ref.
Electron Donor (D)	Electron Acceptor (A)								
C <sub>2</sub> H <sub>4</sub>	O <sub>2</sub>	CO <sub>2</sub>	Pt	β"-Al <sub>2</sub> O <sub>3</sub>	180–300	5x10 <sup>4</sup>	0.25	-30	3, 60
CO	O <sub>2</sub>	CO <sub>2</sub>	Pt	β"-Al <sub>2</sub> O <sub>3</sub>	300–450	1x10 <sup>5</sup> -1x10 <sup>5</sup>	0.3 8	-30 250	3, 61
H <sub>2</sub>	C <sub>6</sub> H <sub>6</sub>	C <sub>6</sub> H <sub>12</sub>	Pt	β"-Al <sub>2</sub> O <sub>3</sub>	100–150	-	-0	-10	13, 62
H <sub>2</sub>	C <sub>2</sub> H <sub>2</sub>	C <sub>2</sub> H <sub>4</sub> , C <sub>2</sub> H <sub>6</sub>	Pt	β"-Al <sub>2</sub> O <sub>3</sub>	100–300	-	-*	-	63
C <sub>2</sub> H <sub>4</sub>	NO	CO <sub>2</sub> , N <sub>2</sub> , N <sub>2</sub> O	Pt	β"-Al <sub>2</sub> O <sub>3</sub>	280–400	-	∞	500	12
CO	NO	CO <sub>2</sub> , N <sub>2</sub> , N <sub>2</sub> O	Pt	β"-Al <sub>2</sub> O <sub>3</sub>	320–400	-	13*	200	64–66
C <sub>3</sub> H <sub>6</sub>	NO	CO <sub>2</sub> , N <sub>2</sub> , N <sub>2</sub> O	Pt	β"-Al <sub>2</sub> O <sub>3</sub>	375	-	10	-	65–67
H <sub>2</sub>	NO	N <sub>2</sub> , N <sub>2</sub> O	Pt	β"-Al <sub>2</sub> O <sub>3</sub>	360–400	-	30	6000	68
H <sub>2</sub>	C <sub>2</sub> H <sub>2</sub> , C <sub>2</sub> H <sub>4</sub>	C <sub>2</sub> H <sub>4</sub> , C <sub>2</sub> H <sub>6</sub>	Pd	β"-Al <sub>2</sub> O <sub>3</sub>	70–100	-	0.13	-	69
C <sub>2</sub> H <sub>4</sub>	O <sub>2</sub>	C <sub>2</sub> H <sub>4</sub> O, CO <sub>2</sub>	Ag	β"-Al <sub>2</sub> O <sub>3</sub>	240–280	-	-	40	70
CO	O <sub>2</sub>	CO <sub>2</sub>	Ag	β"-Al <sub>2</sub> O <sub>3</sub>	360–420	-	2	-	3
C <sub>2</sub> H <sub>4</sub>	O <sub>2</sub>	CO <sub>2</sub>	Pt	Na <sub>3</sub> Zr <sub>2</sub> Si <sub>2</sub> PO <sub>12</sub>	430	-	10	300	71

5. EP studies utilizing K<sup>+</sup> conductors

Reactants		Products	Catalyst	Solid Electrolyte	T (°C)	$\Lambda_{\max(>0)}$ or $\Lambda_{\min(<0)}$	$\rho_{\max(>1)}$ or $\rho_{\min(<1)}$	$PI_{K^+}$	Ref.
Electron Donor (D)	Electron Acceptor (A)								
NH <sub>3</sub>		N <sub>2</sub> , H <sub>2</sub>	Fe	K <sub>2</sub> Zr(PO <sub>4</sub> ) <sub>3</sub>	500–700	-	4.5	-	72

6. EP studies utilizing H<sup>+</sup> conductors

Reactants		Products	Catalyst	Solid Electrolyte	T (°C)	$\Lambda_{\max(>0)}$ or $\Lambda_{\min(<0)}$	$\rho_{\max(>1)}$ or $\rho_{\min(<1)}$	$PI_{H^+}$	Ref.
Electron Donor (D)	Electron Acceptor (A)								
C <sub>2</sub> H <sub>4</sub>	O <sub>2</sub>	CO <sub>2</sub>	Pt	CaZr <sub>0.9</sub> In <sub>0.1</sub> O <sub>3a</sub>	385–470	-3x10 <sup>4</sup>	5	-	73
H <sub>2</sub>	N <sub>2</sub>	NH <sub>3</sub>	Fe	CaZr <sub>0.9</sub> In <sub>0.1</sub> O <sub>3-a</sub>	440	6	∞	6	74
NH <sub>3</sub>		N <sub>2</sub> , H <sub>2</sub>	Fe	CaZr <sub>0.9</sub> In <sub>0.1</sub> O <sub>3-a</sub>	530–600	150	3.6	-	72
CH <sub>4</sub>		C <sub>2</sub> H <sub>6</sub> , C <sub>2</sub> H <sub>4</sub>	Ag	SrCe <sub>0.95</sub> Yb <sub>0.05</sub> O <sub>3</sub>	750	-	8*	10	3, 75
H <sub>2</sub>	C <sub>2</sub> H <sub>4</sub>	C <sub>2</sub> H <sub>6</sub>	Ni	CsHSO <sub>4</sub>	150–170	300	2	12	3, 10
H <sub>2</sub>	O <sub>2</sub>	H <sub>2</sub> O, C <sub>4</sub> H <sub>10</sub>	Pt	Nafion	25	20	6	5	76
1-C <sub>4</sub> H <sub>8</sub>		2-C <sub>4</sub> H <sub>8</sub> (cis, trans)	Pd	Nafion	70	-28	40*	-	14

## 7. EP studies utilizing aqueous alkaline solutions

Reactants		Products	Catalyst	Solid Electrolyte	T (°C)	$\Lambda_{\max(>0)}$ or $\Lambda_{\min(<0)_x}$	$\rho_{\max(>1)}$ or $\rho_{\min(<1)}$	$PI_{OH^-}$	Ref.
Electron Donor (D)	Electron Acceptor (A)								
H <sub>2</sub>	O <sub>2</sub>	H <sub>2</sub> O	Pt	H <sub>2</sub> O – 0.1N KOH	25–50	20	6	20	3, 77, 78

## 8. EP studies utilizing molten salts

Reactants		Products	Catalyst	Solid Electrolyte	T (°C)	$\Lambda_{\max(>0)}$ or $\Lambda_{\min(<0)_x}$	$\rho_{\max(>1)}$ or $\rho_{\min(<1)}$	Ref.
Electron Donor (D)	Electron Acceptor (A)							
SO <sub>2</sub>	O <sub>2</sub>	SO <sub>3</sub>	Pt	V <sub>2</sub> O <sub>5</sub> -K <sub>2</sub> SO <sub>4</sub>	350–450	-100	6	79

\*: Change in product selectivity observed.

#: 4.5 mol% Y<sub>2</sub>O<sub>3</sub> – 10 mol% TiO<sub>2</sub> – 85.5 mol% ZrO<sub>2</sub>

After the establishment via the use of surface spectroscopy (XPS [80,81], UPS [82], TPD [83], PEEM [84], STM [85], work function measurements [86]) but also electrochemistry (cyclic voltammetry [83], potential programmed reduction [87] AC, impedance spectroscopy [36, 88]) that electrochemical promotion is due to the potential-controlled migration (reverse spillover or backspillover) [3] of promoting ionic species ( $O^{2-}$ ,  $Na^+$ ,  $H^+$ ,  $F^-$ ) from the solid electrolyte to the gas exposed catalyst surface, it became clear that electrochemical promotion is functionally very similar to classical promotion and that the promotional index  $PI_P$ , already defined in Equation (2):

$$PI_P = (\Delta r/r_0)/\Delta\theta_P \quad (2)$$

can be used interchangeably both in classical and in electrochemical promotion.

As already mentioned, one important operational difference between classical and electrochemical promotion is that in the latter case one can control in situ, via the applied potential, the coverage of the promoting species on the catalyst surface. Aside from the potential practical significance of such in situ tuning of the catalytic activity on a working catalyst, there is a second advantage for the fundamental study of promotion. One can now examine in situ, i.e. under constant gaseous composition, the effect of the coverage of the promoting species on the catalytic rate in an efficient and systematic manner.

Another important operational advantage of electrochemical promotion is that, if the promoting species lifetime,  $\tau_{PR}$ , on the catalyst surface is too short for any realistic classical promotion application (i.e. if  $\tau_{PR}$  is of the order of hours or min or even sec) one can still use it by continuously replenishing it on the catalyst surface at a rate  $I/nF$ , where  $n$  is the ion charge. In this case the current,  $I$ , must be chosen to satisfy the equation:

$$I/nF = N_G/\tau_{PR} \quad (10)$$

where  $N_G$ , in mol, is the catalyst surface area. In this way some extremely effective but short-lived promoting species, such as  $O^{2-}$  originating from  $Y_2O_3$ -stabilized- $ZrO_2$  (YSZ) or  $TiO_2$  [2,3], and which were totally unknown from classical promotion studies [1], can now be utilized in a continuous and efficient manner.

Another important parameter in electrochemical promotion studies is the characteristic rate relaxation time,  $\tau$ , needed for the catalytic rate to reach steady-state upon imposition of a constant current (galvanostatic transient). As one would expect and as experiment has clearly shown [2,3],  $\tau$  is always of the order  $2FN_G/I$  (Fig. 2):

$$\tau \approx 2FN_G/I \quad (11)$$

The parameter  $2FN_G/I$  expresses the time required to form a monolayer of  $O^{2-}$  on a catalyst surface with  $N_G$

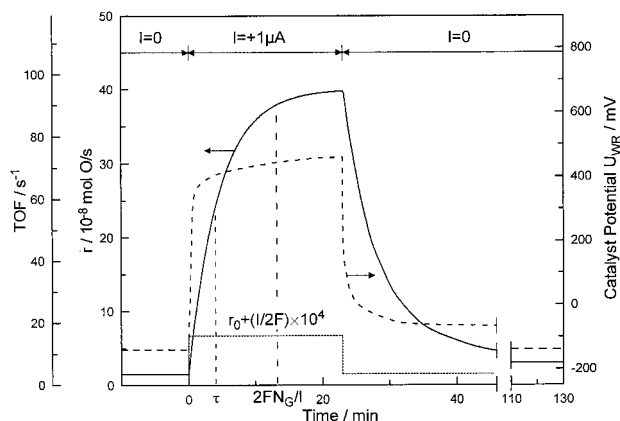


Figure 2. Electrochemical promotion: Rate and catalyst potential response to step changes in applied current during  $C_2H_4$  oxidation on Pt deposited on YSZ, an  $O^{2-}$  conductor.  $T=370^\circ C$ ,  $p_{O_2}=4.6$  kPa,  $p_{C_2H_4}=0.36$  kPa. The catalytic rate increase,  $\Delta r$ , is 25 times larger than the rate before current application,  $r_0$ , and 74000 times larger than the rate  $I/2F$  [19], of  $O^{2-}$  supply to the catalyst.  $N_G$  is the Pt catalyst surface area, in mol Pt, and TOF is the catalytic turnover frequency (mol O reacting per surface Pt mol per s). Reprinted with permission from Academic Press.

sites when  $O^{2-}$  is supplied at a rate  $I/2F$ , as is the case in electrochemical promotion experiments. Equation was the first evidence to suggest that electrochemical promotion is due to the electrochemically controlled migration (backspillover) of promoting  $O^{2-}$  species on the metal catalyst surface [19], a view which has been confirmed by numerous surface spectroscopic techniques [2, 3, 36, 80–88].

### 1.1.3. Metal-support interactions

In commercial catalysts the catalytically active phase is usually dispersed on a highly porous and of high ( $>100$   $m^2/g$ ) surface area support. This high surface area support, also frequently termed carrier, has pores as small as 10 Å and allows for the use of the active phase in a highly dispersed form. The pores are termed macropores when their diameter,  $d$ , is larger than 200 Å. When  $d$  is smaller than 20 Å the pore is termed micropore. IUPAC recommends the term mesopore when  $d$  is between 20 and 200 Å. In most supported commercial catalysts the size of the supported crystallites of the active phase is of the order 10–50 Å (Figure 3). This implies that each crystallite consists of few, typically 10 to 1000, atoms. It also implies that a significant portion of the active phase atoms are on the gas-exposed surface of the crystallites and are thus catalytically active. This portion (percentage) is termed catalyst dispersion,  $D_c$ , and is defined from:

$$D_c = \frac{\text{number of surface catalyst atoms}}{\text{total number of catalyst atoms}} \cdot 100 \quad (12)$$

Since the catalytically active phase is frequently quite expensive (e.g. noble metals) it is clear that it is in

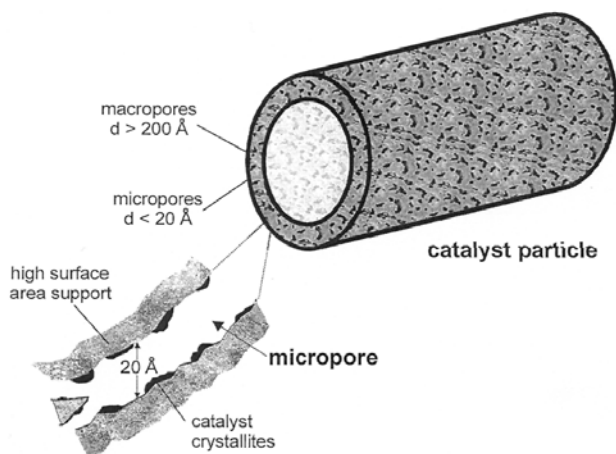


Figure 3. Schematic of a commercial supported catalyst pellet and of one of its micropores.

principle advantageous to prepare catalysts with high, approaching 100%, catalyst dispersion  $D_c$ . This can be usually accomplished without much difficulty by impregnating the porous carrier with an aqueous solution of a soluble compound (acid or salt) of the active metal followed by drying, calcination and reduction [89].

Successful and reproducible preparation of highly dispersed catalysts crucially depends on the state of the carrier surface and on the concentration and pH of the impregnating solution. It is an art and a science for which several good books and reviews exist [89–93].

In the early days of catalysis the porous high surface area support was usually thought to be inert. It soon became obvious, however, that the catalytic activity, or turnover frequency, of a catalytic reaction on a given active phase is quite often seriously affected both by the crystallite size and by the material of the support.

The former phenomenon is usually referred to as "*particle size effect*" and is pronounced for structure sensitive reactions [89,90], i.e. catalytic reactions where the rate and/or selectivity is significantly different from one crystallographic plane to another. Structure sensitive reactions (e.g. isomerizations) frequently occur on catalytic sites consisting of an "ensemble" of surface atoms with specific geometry. It is thus reasonable to expect that, as the active phase crystallite size decreases, there will be a different distribution of crystallographic planes on the catalyst surface, with the possible disappearance of "ensemble" sites, so that both the catalyst activity and selectivity will be significantly affected. On the other hand *structure insensitive*, also termed *facile* [89,90], reactions (e.g. most hydrogenations, some oxidations) are little affected by particle size effects.

The second phenomenon, i.e. the change in catalytic activity or selectivity of the active phase with varying catalyst support, is usually termed *metal-support interaction*. It manifests itself even when the active phase has the same dispersion or average crystallite size on different supports. Metal-support

interactions can influence in a very pronounced way the catalytic and chemisorptive properties of metal and metal oxide catalysts. Typical and spectacular examples are:

a. The phenomenon of strong metal support interactions (SMSI) discovered by Tauster et al. [94] which attracted worldwide attention for many years [95].

b. The effect of dopant-induced-metal support interactions (DIMSI) studied for years by Verykios and coworkers [96].

c. The relatively recent discovery of the highly active Au/SnO<sub>2</sub> oxidation catalysts by Haruta and coworkers [97–99].

In all these cases the support has a dramatic effect on the activity and selectivity of the active phase. In classical terminology [89] all these are Schwab effects "*of the second kind*" where an oxide affects the properties of a metal. Schwab effects "*of the first kind*", where a metal affects the catalytic properties of a catalytic oxide, are less common although in the case of the Au/SnO<sub>2</sub> oxidation catalysts [97,98] it appears that most of the catalytic action takes place near the metal-oxide-gas three phase boundaries.

The nature of metal-support interactions has been the focal point of extensive research and dispute, particularly after the discovery by Tauster et al. [94] of the phenomenon of strong metal-support interactions (SMSI). Although particle-size effects and electronic interactions between the metal particles and the support have been known for years to play a role, the SMSI effect was finally shown to be due to migration of ionic species from the support onto the catalyst particle surface ("decoration") [95]. There have been some interesting recent experimental and theoretical advances [100–107], but a thorough understanding of metal-support interactions is one of the greatest challenges in heterogeneous catalysis.

Although SiO<sub>2</sub> and  $\gamma$ -Al<sub>2</sub>O<sub>3</sub> are the most common high surface area industrial catalyst supports (considered in general to give rise to weak metal-support interactions), in recent years there has been an increasing tendency to replace these supports for numerous catalytic applications, mostly oxidations, but also NO reduction, with TiO<sub>2</sub> or CeO<sub>2</sub> or ZrO<sub>2</sub>-based porous supports [108]. Little information exists in the open literature as to why this gradual substitution is taking place [105,109] but it is common understanding that these supports, generally believed to lead to stronger metal-support interactions, result in increased activity [105,109], selectivity and useful lifetime of the metal particles deposited on them.

The extent of metal-support interactions for a given catalytic system can again be quantified by defining a metal-support interaction rate enhancement ratio,  $p_{MSI}$ , from:

$$p_{MSI} = r/r_0 \quad (13)$$

where  $r_0$  is the catalytic rate per unit surface area of the active catalyst in its unsupported form and  $r$  is the same

catalytic rate per unit surface area of the supported catalyst.

Clearly  $\rho_{\text{MSI}}$  is expected to vary from one support to another even for facile reactions, while for structure sensitive reactions  $\rho_{\text{MSI}}$  can be reasonably expected to be a function not only of the support but also of the particle size of the active phase.

Figure 4 shows measured  $\rho_{\text{MSI}}$  values for the case of  $\text{C}_2\text{H}_4$  oxidation on finely dispersed (0.5 wt%) Rh on five different supports:  $\rho_{\text{MSI}}$  values exceeding 100 are obtained for this interesting system. As we shall see, the

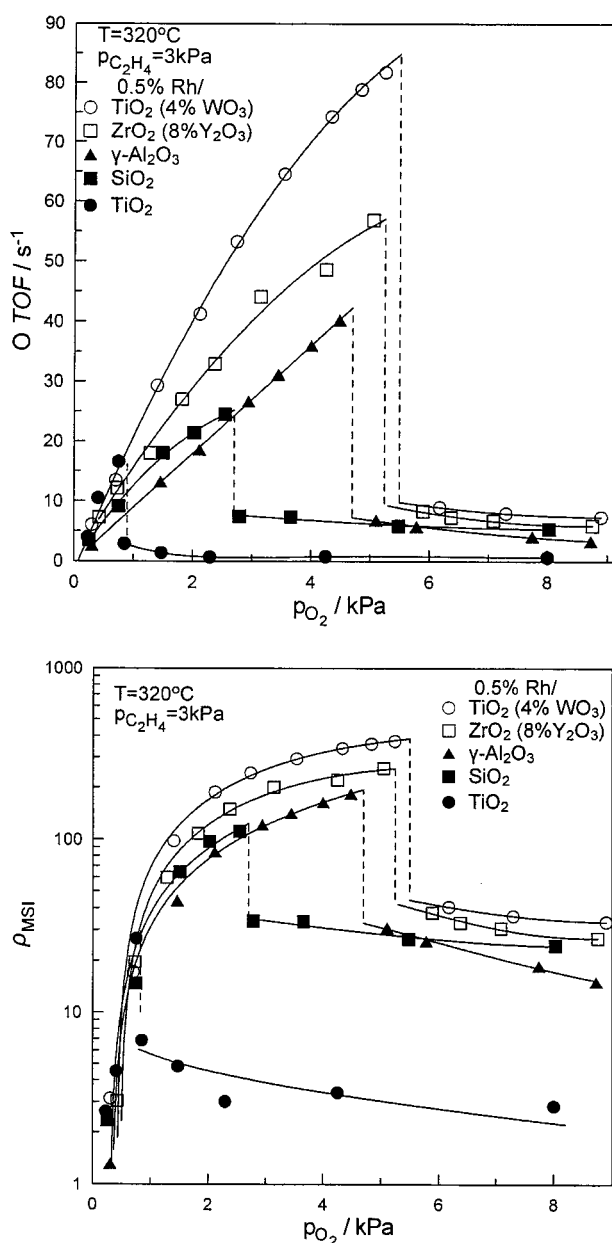


Figure 4. (top) Effect of  $p_{\text{O}_2}$  on the rate (TOF) of  $\text{C}_2\text{H}_4$  oxidation on Rh supported on five supports of increasing  $\Phi$ . Catalyst loading 0.5wt%. [135,140] (bottom) Effect of  $p_{\text{O}_2}$  on the metal-support interactions rate enhancement ratio,  $\rho_{\text{MSI}}$ . Reprinted with permission from Elsevier Science.

sequence of increasing activity of the five supports coincides with the sequence of their absolute potentials or work functions.

#### 1.1.4. Spillover-backspillover phenomena

The effect of spillover plays an important role in heterogeneous catalysis and was extensively studied during recent years. It was first noticed in the 1950s by Kuriacose [110]. Work in this area has been reviewed by Teichner [111] and by Conner et al. [112].

The spillover effect can be described as the mobility of sorbed species from one phase on which they easily adsorb (donor) to another phase where they do not directly adsorb (acceptor). In this way a seemingly inert material can acquire catalytic activity. In some cases, the acceptor can remain active even after separation from the donor. Also, quite often, as shown by Delmon and coworkers [113–115], simple mechanical mixing of the donor and acceptor phases is sufficient for spillover to occur and influence catalytic kinetics leading to a Remote Control mechanism, a term first introduced by Delmon [113]. Spillover may lead, not only to an improvement of catalytic activity and selectivity but also to an increase in lifetime and regenerability of catalysts. Although spillover of reactants (e.g. H, O) can play unimportant role in some catalytic systems, in recent years it is becoming clear that spillover and backspillover of promoters (e.g.  $\text{O}^{2-}$ ,  $\text{Na}^+$ ) from one phase to another is a far more important phenomenon [2].

#### 1.2. Work function of surfaces, electropositive and electronegative promoters

The work function,  $\Phi$ , of solid surface, in eV/atom, is the minimum energy which an electron must have in order to escape from the Fermi level,  $E_F$ , of that solid through that surface, when the surface is electrically neutral, to a distance of a few  $\mu\text{m}$  outside the surface so that image charge forces are negligible:

$$\Phi = -E_F (= -\bar{\mu}) \quad (14)$$

where  $\bar{\mu}$  is the electrochemical potential of electrons in the solid. The latter always equals ( $\bar{\mu} = E_F$ ) the Fermi level of the solid [2, 3, 116–119].

When the solid surface under consideration carries a net charge, then the work function ( $\Phi$ ) and electrochemical potential  $\bar{\mu}$  (or Fermi level  $E_F$ ) are related via (Fig. 5)

$$-\bar{\mu} = \Phi + e\Psi \quad (15)$$

where  $\Psi$  is the outer (Volta) potential of the surface. The energy  $e\Psi$  is known to surface physicists as the "vacuum level". Equation presents the surface science approach of counting the energy difference between the zero energy state of electrons (always taken in this

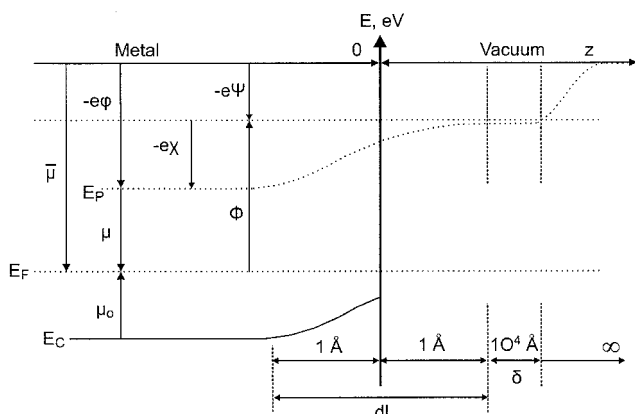


Figure 5. Schematic representation of the definitions of work function  $\Phi$ , chemical potential of electrons  $\mu$ , electrochemical potential of electrons or Fermi level  $\bar{\mu} = E_F$ , surface potential  $\chi$ , Galvani (or inner) potential  $\phi$ , Volta (or outer) potential  $\Psi$ , Fermi energy  $\mu_0$  and of the variation in the mean effective potential energy  $E_P$  of electrons in the vicinity of a metal-vacuum interface according to the jellium model.  $E_C$  is the energy at the bottom of the conduction band and  $dl$  denotes the double layer at the metal-vacuum interface.

Chapter as the energy of an electron at its ground state and "infinite" distance from any solid (Fig. 5). There is a second, electrochemical, way of counting this energy difference:

$$\bar{\mu} = \mu + (-e)\phi \quad (16)$$

where  $\mu$  is the chemical potential of electrons in the metal and the inner or Galvani potential,  $\phi$ , is the electrostatic potential of electrons in the solid.

The surface science approach (Eq. (15)) has the important advantage that both  $\Phi$  and  $\Psi$  are measurable quantities. This is not the case for the electrochemical approach (Eq. (16)) since neither  $\mu$  nor  $\phi$  are absolutely measurable quantities. Only changes in  $\phi$  are measurable [3].

The quantities  $\bar{\mu}$ ,  $\mu$  and  $\phi$  are bulk properties of the metal [2, 116–119]. The quantities  $\Phi$ , and of course  $\Psi$ , are surface properties which can vary on metal surfaces from one crystallographic plane to the other. Such variations are typically on the order of 0.1 eV but can be as high as 0.5 eV. The measured work function,  $\Phi$ , of a polycrystalline metal is an average of the  $\Phi$  values for different crystallographic planes [2,3].

The work function of clean metal surfaces, which we denote by  $\Phi_0$ , varies between 2 eV for alkalis up to 5.5 eV for transition metals such as Pt. In general it increases as one moves to the right on the periodic table [120] but deviations exist (Fig. 6).

When atoms or molecules (e.g. promoters or reactant adsorbates) adsorb on a metal surface they change its work function. Electronegative (electron acceptor) adsorbates such as O or Cl can increase the  $\Phi$  of a metal surface up to 1 eV. Electropositive (electron donor) adsorbates such as hydrocarbons or, particularly, alkalis can decrease the  $\Phi$  of a metal surface up to 3 eV.

Thus depending on the change a promoter induces on the work function,  $\Phi$ , of a catalyst surface, a major distinction can be made between *electropositive (electron donor)* and *electronegative (electron acceptor)* promoters.

In the same way, catalytic reactant adsorbates, and thus catalytic reactants, can be divided into *electron donor* and *electron acceptor* adsorbates or reactants. Hydrocarbons, and in particular unsaturated ones, always behave as electron donors (D), while O, Cl, and in most cases CO and NO, behave as electron acceptors. Adsorbates, such as H, CO and NO which, depending on the catalyst surface and the nature of the other coadsorbates, can change their behaviour between electron donor and electron acceptor, are called amphoteric adsorbates [2, 3, 121, 122].

The variation in  $\Phi$  of a metal with the coverage  $\theta$  of an adsorbate, promoter or adsorbed reactant, is described by the Helmholtz equation:

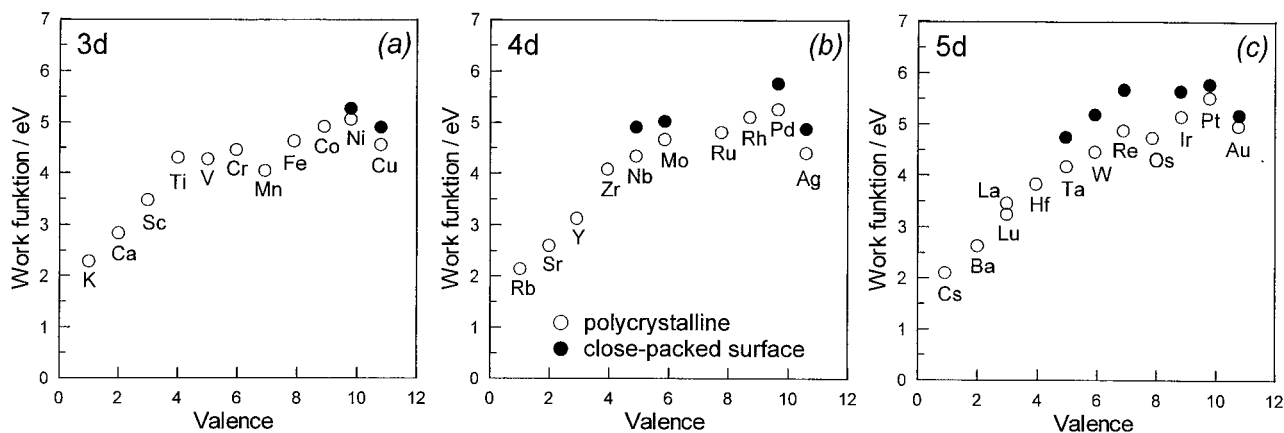


Figure 6. Experimental work function values,  $\Phi_0$ , for the 3d, 4d and 5d series including the alkali, alkaline-earth, and noble metals for polycrystalline surfaces (open circles) and for single crystal surfaces (filled circles). [120] Reprinted with permission from the American Physical Society.

$$\Delta\Phi = \frac{eN_M}{\epsilon_0} \Delta P_j \theta_j \quad (17)$$

where  $e$  is the electron charge ( $1.6 \cdot 10^{-19}$  C),  $N_M$  is the surface atom density ( $\text{atom}/\text{m}^2$ ),  $\epsilon_0$  is the electric permeability of vacuum ( $\epsilon = 8.85 \cdot 10^{-12}$  C<sup>2</sup>/Jm) and  $P_j$  (Cm) is the dipole moment of the adsorbate  $j$  in the adsorbed state. Typically  $P_j$  is of the order of  $10^{-29}$  Cm or 3D (Debye). The Debye unit, D, equals  $3.36 \cdot 10^{-30}$  Cm. The dipole moments of adsorbates are taken by convention positive in this paper when the adsorbate dipole vector,  $\vec{P}_j$ , is pointing to the vacuum (electronegative adsorbates, e.g.  $\text{O}^{\delta-}$ ,  $\text{Cl}^{\delta-}$ ) and negative when  $\vec{P}_j$  is pointing to the surface (electropositive adsorbates, e.g.  $\text{Na}^{\delta+}$ ).

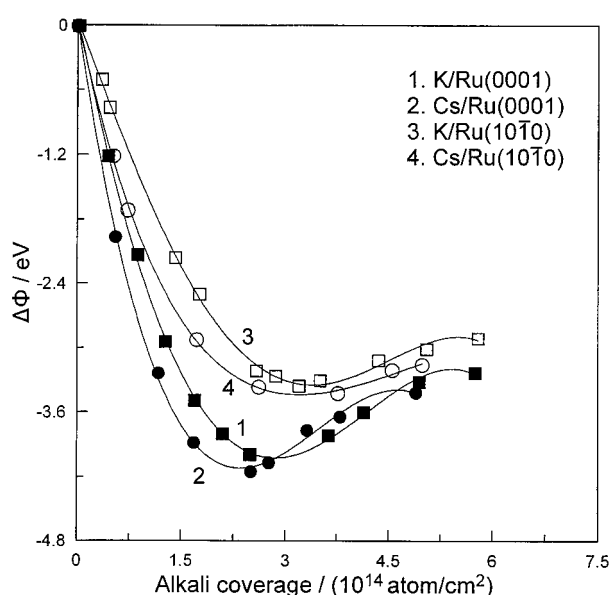


Figure 7. Work function changes,  $\Delta\Phi$ , as a function of K and Cs coverages for Ru(0001) (1 and 2) and for Ru (10  $\bar{1}$  0) (3 and 4) [123]. Reprinted with permission from Springer-Verlag GmbH & Co.

### 1.3. Basic promoter selection criteria

In selecting a promoter for classical (chemical) promotion of a catalytic reaction two necessary, but not sufficient, criteria must be satisfied [121,122]:

a. The promoter must not be consumed in the catalytic reaction and must not be deactivated by the reactants and products.

b. The promoter must have a large absolute dipole moment value,  $|P_j|$ , so that large variations,  $\Delta\Phi$ , in the catalyst work function,  $\Phi$ , can be induced by relatively small coverages,  $\theta_j$ , of the promoter (Eq. (17)). The latter is necessary in order to minimize site-blocking effects caused by high promoter coverage.

Alkali metals satisfy both of these criteria [123,124] as can be seen in Figures 7 and 8. Due to their absolutely large dipole moments,  $|P_{\text{alk}}| \approx 5\text{--}10$  D, alkali coverages,  $\theta_{\text{alk}}$ , of the order of 0.1 suffice to decrease the catalyst work function  $\Phi$  by more than 2.5 eV.

Which types of catalytic reactions can be promoted (accelerated) by such a pronounced decrease in catalyst work function? They are called *electrophilic* and we will discuss them in the next section, together with their counterpart, *electrophobic* reactions, which are promoted by increasing catalyst work function.

### 1.4. Effect of promoters on chemisorption

What is the mechanism of the promoting action? To start discussing this we can first focus on Figure 8 and observe that as the alkali coverage,  $\theta_{\text{alk}}$ , is increased, the alkali dipole moment decreases and so does also the alkali chemisorptive bond strength  $E_d$ . This weakening in the alkali chemisorptive bond strength is, to a large extent, due to *repulsive lateral interactions* between the adsorbed, partly positively charged, alkali atoms.

In fact, as can be seen in Figure 8, upon crossplotting  $E_d$  vs the work function change,  $\Delta\Phi$ , induced by the alkali adatoms, a straight line with a positive slope is obtained. For non-activated adsorption,

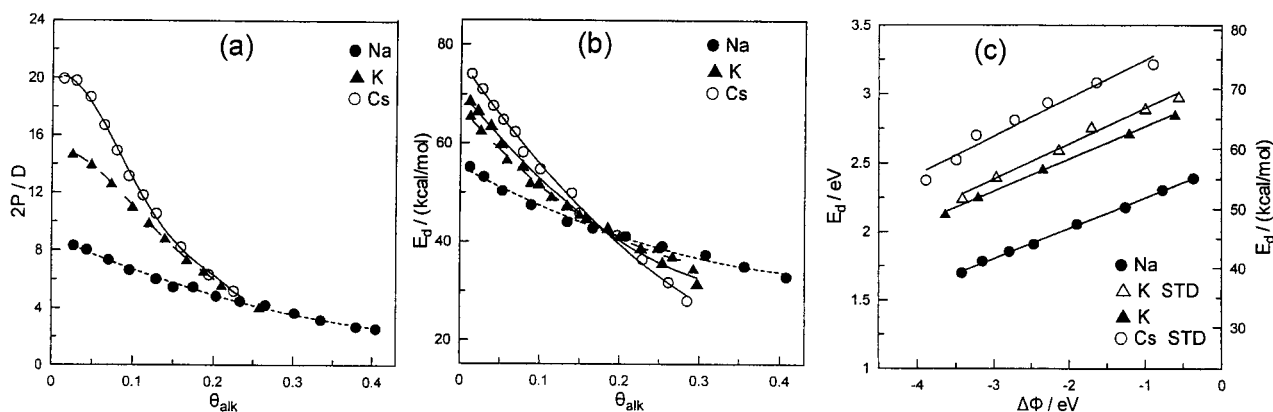


Figure 8. Effect of alkali coverage on (a) the alkali adatom dipole moment and alkali desorption energy (b) for Na, K and Cs adsorbed on Ru (0001) and corresponding effect of work function change  $\Delta\Phi$  on the alkali desorption energy (c). [124] Reprinted with permission from Elsevier Science.

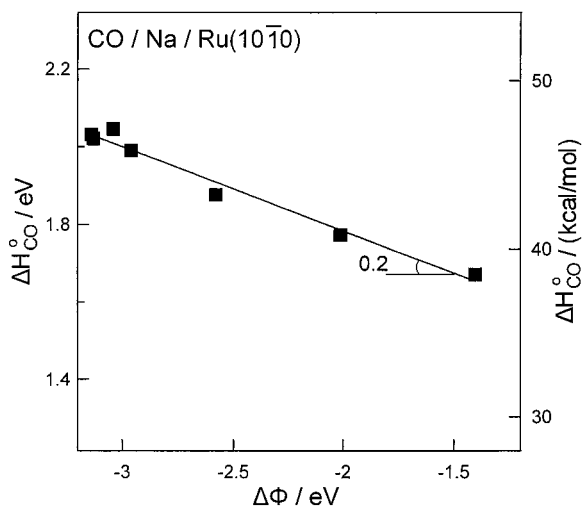


Figure 9. Dependence of the initial heats of CO adsorption,  $\Delta H_{CO}^0$ , on the alkali coverage, as estimated from the CO TPD spectra at very low CO coverages assuming invariable frequency factor [125,126] (a) and on the corresponding work function change  $\Delta\Phi$  [125,126] (b). Reprinted with permission from Elsevier Science.

as is the case here, this implies a linear decrease in the heat of chemisorption of the alkali atoms [ $\Delta H_{adl}$  ( $=E_d$ )] with decreasing  $\Phi$ :

$$\Delta[\Delta H_{adl}] = \alpha_H \Delta\Phi \quad (18)$$

where the parameter  $\alpha_H$  has in this case a value near 0.25. This equation is of rather broad significance as it approximates, in most cases with reasonable accuracy [2,122], the observed variation in heats of adsorption of adsorbates (promoters but also catalytic reactants and products) with varying  $\Phi$ .

Another example of Equation is shown in Figure 9 which depicts the effect of  $\Delta\Phi$ , induced by varying the coverage of Na [125,126], on the heat of chemisorption of CO which, in presence of alkalis, always behaves as an electron acceptor. Here  $\alpha_H$  is negative and equals -0.2.

Equation (18) is in good agreement with recent rigorous quantum mechanical calculations using metal clusters [127,128] and can also be derived, as shown elsewhere [121] and as we will see in the next section, by simply taking into account the electrostatic ("through the vacuum") lateral interactions in the adsorbed layer.

The parameter  $\alpha_H$  is positive for electropositive (electron donor) adsorbates and negative for electronegative (electron acceptor) adsorbates. Even when deviations from linearity exist, the main features of Equation (18) remain valid and form the *basis* for understanding the *main kinetic features of classical and electrochemical promotion* [2,3,122]:

*Increasing catalyst work function causes an increase in the heat of adsorption (thus chemisorptive bond strength) of electropositive (electron donor) adsorbates and a decrease in the heat of adsorption*

*(thus chemisorptive bond strength) of electronegative (electron acceptor) adsorbates.*

As a corollary of the above general chemisorption promotional rule, the following two rules are immediately derived [2,122]:

*Rule C1: Electropositive adsorbates strengthen the chemisorptive bond of electron acceptor (electronegative) adsorbates and weaken the chemisorptive bond of electron donor (electropositive) adsorbates.*

*Rule C2: Electronegative adsorbates weaken the chemisorptive bond of electron acceptor (electronegative) adsorbates and strengthen the chemisorptive bond of electron donor (electropositive) adsorbates.*

These rules must be supplemented by the following two "amphoteric" rules [2,122], which supplement the definition of electron acceptor and electron donor adsorbates.

*Rule C3: In presence of a strong electron donor (electropositive) adsorbate (e.g. K, Na) a weaker electron donor (e.g. NO on Pt(111)) behaves as an electron acceptor.*

*Rule C4: In a presence of a strong electron acceptor (electronegative) adsorbate (e.g. O) a weaker electron acceptor (e.g. CO on Ni(111)) behaves as an electron donor.*

There are two molecular mechanisms which lead to the above rules:

Direct electrostatic ("through the vacuum") dipole attraction or repulsion which, in the case of attraction, may lead even to surface compound formation.

Indirect ("through the metal") interaction due to the redistribution of electrons in the metal. In this case an electropositive promoter decreases the work function of the surface and this in turn weakens the chemisorptive bond of electropositive (electron donor) adsorbates and strengthens the chemisorptive bond of electronegative (electron acceptor) adsorbates.

The extent of the contribution of each of these two mechanisms varies from one system to the other as recent quantum mechanical calculations have shown [127,128]. In either case, however, linear variations are often obtained in the change in heat of adsorption vs the change in the work function, with slopes on the order of  $\pm 1$ , in good agreement with experiment [2,121].

## 1.5. Promotional kinetics and rules

Upon varying the coverage of a promoter on a catalyst surface, one is varying the catalyst work function  $\Phi$  (in the negative direction when the promoter is electropositive and in the positive direction when the promoter is electronegative). As one might expect, such a variation in promoter coverage leads to four main types of catalytic rate,  $r$ , vs  $\Phi$  behaviour (Fig. 10) [2,121,122] where  $p_A$  and  $p_D$  denotes the partial

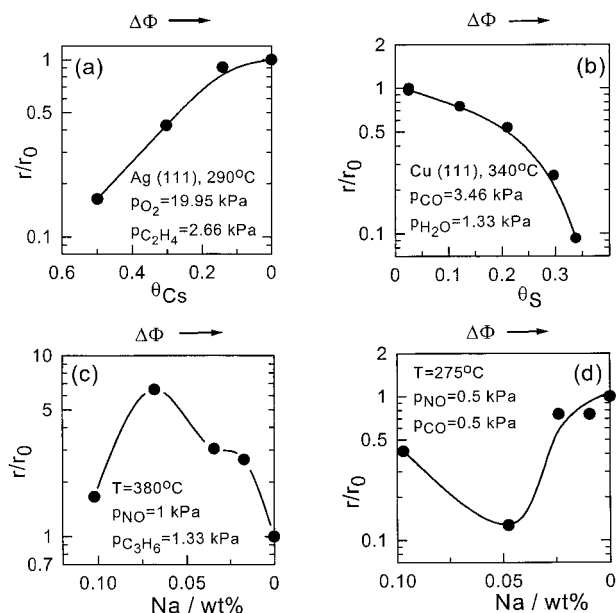


Figure 10. Examples for the four types of global classical promotion behaviour. Work function increases with the x-axis. (a) Steady-state (low conversion) rates of ethylene oxide (EtO) and  $\text{CO}_2$  production from a mixture of 20 torr of ethylene and 150 torr of  $\text{O}_2$  for various Cs predosed coverages on Ag(111) at 563 K [141] (b) Rate of water-gas shift reaction over Cu(111) as a function of sulphur coverage at 612 K, 26 Torr CO and 10 Torr  $\text{H}_2\text{O}$  [142] (c) Effect of sodium loading on NO reduction to  $\text{N}_2$  by  $\text{C}_3\text{H}_6$  on Pd supported on YSZ [143] at  $T=380^\circ\text{C}$  (d) Effect of sodium loading on the rate of NO reduction by CO on Na-promoted 0.5 wt% Rh supported on  $\text{TiO}_2(4\% \text{WO}_3)$  [144].

pressures of the electron acceptor (A) and electron donor (D) reactants:

1. Purely electrophobic,  $\partial r/\partial \Phi_{P_A, P_D} > 0$
2. Purely electrophilic,  $\partial r/\partial \Phi_{P_A, P_D} < 0$
3. Volcano type (r exhibits a maximum at a value  $\Phi_M$ )
4. Inverted volcano-type (r exhibits a minimum at a value  $\Phi_m$ )

Can we predict a priori which one of the above four types of global r vs  $\Phi$  behaviour a given catalytic reaction will exhibit? The answer, as shown recently [2,121,122], is yes, provided we know the kinetics (i.e. the r vs  $p_A$  and  $p_D$  dependence) on the unpromoted surface!

The corresponding rules are valid both for classical (chemical) and electrochemical promotion and are intimately related to the previously discussed chemisorption promotional rules. Their extraction became possible due to the easy, continuous and systematic experimental  $\Phi$  variation which electrochemical promotion offers [2,121,122].

A summary of the rules is the following:

**G1. Purely electrophobic behaviour is obtained when A is very strongly adsorbed on the catalyst surface.**

**G2. Purely electrophilic behaviour is obtained when D is very strongly adsorbed on the catalyst surface.**

**G3. Volcano-type behaviour is obtained when both A and D are strongly adsorbed on the catalyst surface.**

**G4. Inverted volcano-type behaviour is obtained when both A and D are weakly adsorbed on the catalyst surface.**

More than sixty examples of the above rules have been discussed [2,121,122]. These rules enable one, in a straightforward manner, to formulate the following three practical rules for promoter selection with respect to rate maximization [2,121].

**Rule P1:** If a catalyst surface is predominantly covered by an electron acceptor adsorbate, then an electron acceptor (electronegative) promoter is to be recommended.

**Rule P2:** If a catalyst surface is predominantly covered by an electron donor adsorbate, then an electron donor (electropositive) promoter is to be recommended.

**Rule P3:** If a catalyst surface has very low coverages of both electron acceptor and electron donor adsorbates, then both an electron acceptor and electron donor promoter will enhance the rate.

Needless to remind that the above practical promotional rules are applicable for modest (e.g.  $< 0.2$ ) coverages of the promoting species so that site-blocking by the promoter does not become the dominant factor limiting the catalytic rate [2,121].

### 1.5.1.1. Work function measurements

One of the first key steps in understanding the origin of electrochemical promotion was the realization that solid electrolyte cells with metal electrodes are both work function probes and work function controllers for the gas-exposed surfaces of their electrodes (Fig. 11):

$$eU_{WR} = \Phi_W - \Phi_R \quad (19)$$

$$e\Delta U_{WR} = \Delta \Phi_w \quad (20)$$

These important equations have been established using both the Kelvin probe (vibrating capacitor) technique [7,129] and UPS [82] (electron cutoff energy). At the molecular level the variation of  $\Phi$  with catalyst-electrode potential  $U_{WR}$  is due to the spillover-backspillover of  $\text{O}^{2-}$  (or  $\text{Na}^+$ ) from the solid electrolyte onto the catalyst/gas interface.

In view of the fact that in any electrochemical cell it is [2,3,129]:

$$eU_{WR} = \bar{\mu}_R - \bar{\mu}_W = \Phi_W - \Phi_R + e\Psi_W - e\Psi_R \quad (21)$$

$$e\Delta U_{WR} = \Delta \Phi_w + e\Delta \Psi_w \quad (22)$$

the experimental Equations (19) and (20) imply that in solid electrolyte cells with ion spillover-backspillover one has:

$$\Psi_W = \Psi_R = C \quad (23)$$

where the constant C vanishes for overall neutral cells [129], which is usually the case. Equation and its

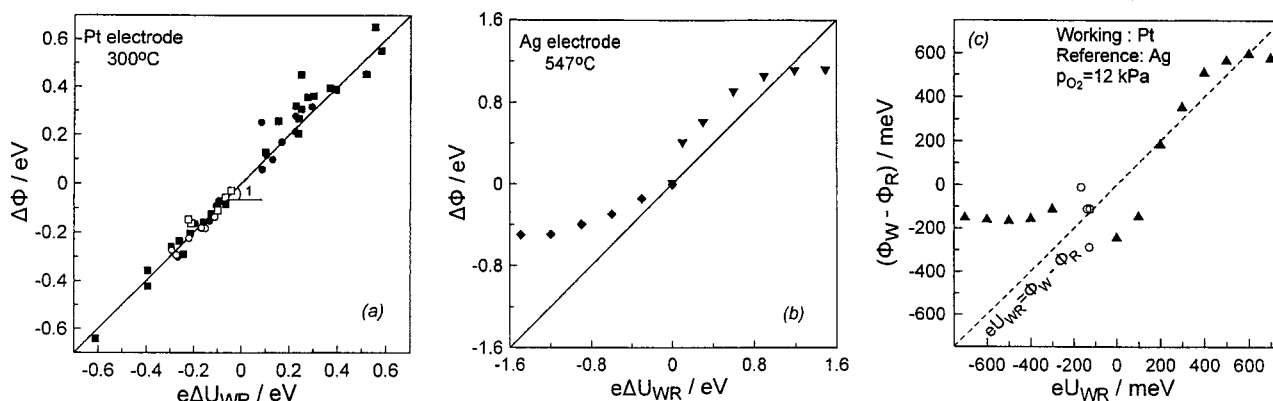


Figure 11. Effect of catalyst–electrode potential  $U_{WR}$  on the work function  $\Phi$  of the gas exposed catalyst–electrode surface (a) Pt/YSZ,  $T = 300^\circ\text{C}$  (squares), Pt/ $\beta''\text{-Al}_2\text{O}_3$ ,  $T = 240^\circ\text{C}$  (circles), filled symbols: closed-circuit operation, open symbols: open-circuit operation,  $\text{O}_2$ ,  $\text{C}_2\text{H}_4/\text{O}_2$  and  $\text{NH}_3/\text{O}_2$  mixtures.[7,86] (b) Ag/YSZ,  $T = 547^\circ\text{C}$ .82 (c) Dependence of  $\Phi_{W(\text{Pt})} - \Phi_{R(\text{Ag})}$  on potential  $U_{WR}$  for the system Pt(W)–Ag(R).[129] Open symbols: Open-circuit operation. Filled symbols: Closed circuit operation  $T = 673\text{ K}$ .

mathematically equivalent Eqs. and, simply reflect the presence of an overall neutral electrochemical double layer at the metal/gas interface [129–131]. This double layer is usually termed *effective double layer* [129–131] and is overall neutral, as every other double layer in electrochemistry (Fig. 12).

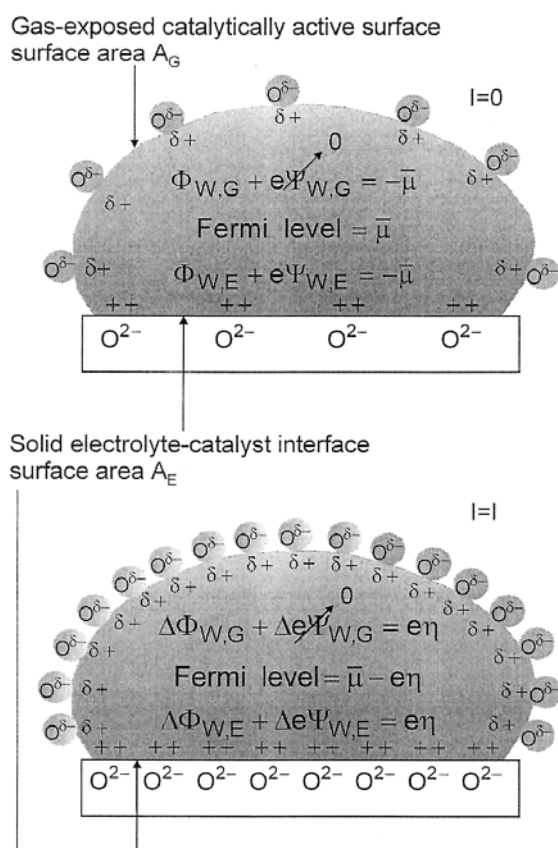


Figure 12. Schematic representation of a metal crystallite deposited on YSZ and of the changes induced in its electronic properties upon polarizing the catalyst–solid electrolyte interface and changing the Fermi level (or electrochemical potential of electrons) from an initial value to a new value  $\bar{\mu} - e\eta$ . [131] Reprinted with permission from Elsevier Science.

The effective double layer concept is an important one, as it shows that electrochemical promotion, but also promotion and also, as we shall see, metal–support–interactions–promoted catalysis, is *catalysis in presence of a double layer* [2]. In the case of electrochemical promotion the double layer is *in situ* controllable.

Equations (19), (20) and (23) are valid both at open-circuit and under closed-circuit, i.e. NEMCA, conditions, in presence or absence of catalytic reactions as long as the effective double layer is present at the metal/gas interface [129].

Deviations from Equations (19), (20) and (23) occur when the effective double layer at the metal/gas interfaces is destroyed.[129] This is the case for (a) very low temperatures ( $<250^\circ\text{C}$  for YSZ,  $>100^\circ\text{C}$  for  $\beta''\text{-Al}_2\text{O}_3$ ) where ion spillover–backspillover is kinetically frozen, or (b) very high temperatures ( $>500^\circ\text{C}$  for YSZ,  $>400^\circ\text{C}$  for  $\beta''\text{-Al}_2\text{O}_3$ ) where the effective double layer desorbs; (c) fast diffusion-controlled catalytic reactions which again destroy the double layer; (d) formation of insulating carbonaceous or oxidic deposits at the metal/gas interface which allow for the storage of net electric charge [129].

Nevertheless the experimental range of stability of the effective double layer and thus validity of Eqs. (19), (20) and (23) is very broad and practically coincides with the range of electrochemical promotion itself.

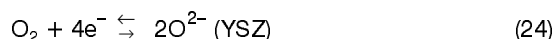
### 1.5.1.2. Absolute potential of supports

Another important consequence of Eq. (19) is that it automatically defines by itself an absolute potential scale in solid state electrochemistry. *The absolute potential is simply the extraction potential,  $\Phi/e$ , of an electrode (any electrode) in contact with the solid electrolyte.* The reference state of the electrons is not that in another (reference) electrode, but rather that of an electron at its ground state outside the electrolyte

surface (or at its ground state at "infinity" as long as the cell is overall neutral, thus  $\Psi=0$ ) [129].

An amazing, yet straightforward, fact is that *the absolute potential does not depend on the electrode material, but is only a property of the electrolyte and of the gas phase* [129]. This is why Frumkin [132] called the absolute potential (in aqueous electrochemistry) energy of solvation of an electron into the electrolyte.

This can be understood easily as follows: Consider the equilibrium:



which takes place not only at the three-phase boundaries (tpb) metal–solid electrolyte–gas but also over the entire metal–gas interface as long as  $\text{O}^{2-}$  backspillover is in equilibrium ( $\bar{\mu}_{\text{O}^{2-}(\text{YSZ})} = \bar{\mu}_{\text{O}^{2-}(\text{M})}$ ). The resulting equilibrium conditions is:

$$\bar{\mu} = \frac{1}{2} \bar{\mu}_{\text{O}^{2-}(\text{YSZ})} - \frac{1}{4} \mu_{\text{O}_2(\text{gas})} \quad (25)$$

where  $\bar{\mu}$  is the electrochemical potential (Fermi level) of electrons in the metal.

As long as the double layer is present at the metal/gas interface, it is  $\Psi = 0$ , thus  $-\bar{\mu} = \Phi$ , thus:

$$U_{\text{abs}} = \Phi/e = \frac{1}{4e} \mu_{\text{O}_2(\text{g})} - \frac{1}{2e} \bar{\mu}_{\text{O}^{2-}(\text{YSZ})} \quad (26)$$

and thus one sees that indeed the absolute potential,  $U_{\text{abs}}$ , is only a property of the electrolyte and of the gaseous oxygen chemical potential [129].

Experiment has shown [129] that for standard conditions in solid state electrochemistry ( $p_{\text{O}_2} = 1 \text{ atm}$ ,  $T=673\text{K}$ ) the corresponding standard absolute potential of YSZ is:

$$U_{\text{abs}}^0 = \Phi^0/e = -\frac{1}{2e} \bar{\mu}_{\text{O}^{2-}(\text{YSZ})} = 5.14 \pm 0.05 \text{ V} \quad (27)$$

This, in view of Eq. (26), means that the standard electrochemical potential of  $\text{O}^{2-}$  in YSZ is:

$$\bar{\mu}_{\text{O}^{2-}(\text{YSZ})} = -10.28 \pm 0.1 \text{ eV / atom} \quad (28)$$

It is thus now clear that one can assign to each  $\text{O}^{2-}$ –conducting support, or to any ionic or mixed ionic–electronic conducting support two new properties, i.e. its *absolute potential* and its *standard absolute potential*. For  $\text{O}^{2-}$  conducting or mixed  $\text{O}^{2-}$ –electronic conductors the defining equations are Eq. (26) and Eq. (27) respectively where the numerical value corresponds to 8 mol%  $\text{Y}_2\text{O}_3$ – $\text{ZrO}_2$  [129].

In view of Equation (27) one may conclude that the more stable  $\text{O}^{2-}$  is in the support (carrier), i.e. the lower  $\bar{\mu}_{\text{O}^{2-}}$  is, the higher is the work function and absolute potential of the support.

It must be emphasized that due to Fermi level pinning ( $\bar{\mu} = E_F$ ) between the metal and the solid electrolyte,  $\bar{\mu}$  in Eq. (25) is also the Fermi level of the support [129]. Thus *the absolute potential of a support, times the unit charge, equals the negative of its Fermi level*.

The importance of these considerations for metal–support interactions with  $\text{ZrO}^{2-}$ ,  $\text{TiO}^{2-}$  and  $\text{CeO}^{2-}$  containing supports is obvious and will be discussed in the last section.

A last practical question: How one can easily measure the absolute potential of a support? The answer is simple: By simply depositing a porous metal (any metal) electrode on it and measuring the work function of the backspillover–modified electrode [129].

### 1.6. Mathematical modeling of promotional kinetics

Recently a rigorous quantitative model has been developed in order to describe promotional and, more generally, catalytic kinetics [122, 133]. The model can be viewed as an extension of classical Langmuir–Hinshelwood–Hougen–Watson (LHHW) kinetics.

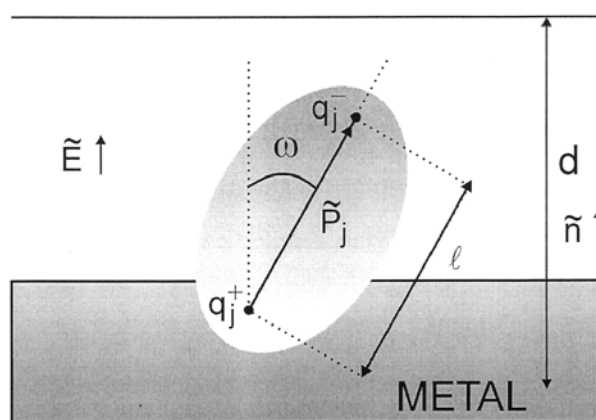
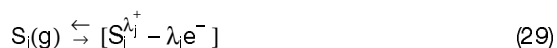


Figure 13. Schematic of an adsorbate, modeled as a dipole, in the presence of the metal/gas effective double layer.

The basis of the model is shown in Figure 13. Each adsorbate is modeled as dipole characterized by the distance,  $\lambda$ , between the positive and negative charge  $q$  and by the partial charge transfer parameter  $\lambda_j$  defined from the equilibrium:



where  $\text{S}_j$  denotes a reactant,  $j$ , and the rhs of Eq. (29) denotes the adsorbate dipole. The dipole interacts with the field strength,  $\tilde{E}$ , of the double layer, so that its electrochemical potential,  $\bar{\mu}_j(\text{ad})$ , can be written as:

$$\bar{\mu}_j(\text{ad}) = \mu_j(\text{ad}) + N_{\text{AV}} \tilde{P}_j \cdot \tilde{E} \quad (30)$$

where  $\mu_j(\text{ad})$  is the chemical potential of the adsorbed species and  $N_{\text{AV}}$  is Avogadro's number.

Assuming uniform adsorption sites and using the fact [2] that:

$$\tilde{E} = (\Delta\Phi/ed) \bar{n} \quad (31)$$

where  $\Delta\Phi$  is the deviation of  $\Phi$  from its value at the point of zero charge (pzc) [2], one obtains the isotherm:

$$k_j p_j = (\theta_j / (1 - \theta_j)) \exp(-\lambda_j \Pi) \quad (32)$$

with

$$\Pi = \Delta\Phi \left( \frac{\lambda}{2d} \cos\omega \right) / k_b T \quad (33)$$

$$k_j = \exp((\mu_j^0(g) - \mu_j^0(ad)) / RT) \quad (34)$$

The first success of the effective double layer isotherm (Eq. (32)) is that it predicts the experimentally observed linear variation of isosteric heat of adsorption or chemisorptive binding energy  $E_j$  with work function  $\Phi$  (Figs. 8, 9, 14, 15):

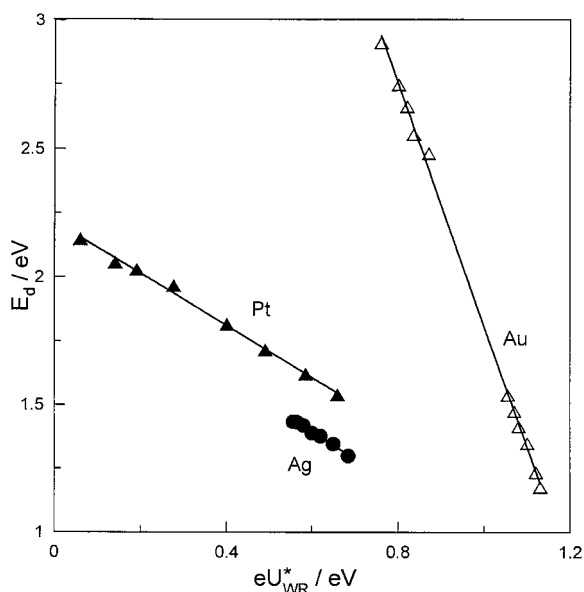


Figure 14. Effect of catalyst potential on the oxygen desorption activation energy,  $E_d$ , calculated from the modified Redhead analysis for Pt, Ag and Au electrodes deposited on YSZ. [145-147] Reprinted from ref. [145] with permission from the Institute for Ionics.

$$E_{b,j} = E_{b,j}^0 + (\lambda_j \lambda / 2d) \Delta\Phi \quad (35)$$

Thus for an electron acceptor adsorbate ( $\lambda_j < 0$ ), Eq. (35) predicts a linear increase in  $E_{b,j}$  with  $\Phi$ , both in excellent agreement with experiment (Figs. 8, 9, 14) and with rigorous cluster quantum mechanical calculations (Fig. 15).

The second, and most important, success of the effective double layer isotherm is that when considering the coadsorption and rate controlling surface reaction of two reactants, A and D, one obtains the following analytical expression for the catalytic rate:

$$r = k_R \theta_D \theta_A = \frac{k_R k_A k_D p_D p_A \exp[(\lambda_D + \lambda_A) \Pi]}{(1 + k_D p_D \exp(\lambda_D \Pi) + k_A p_A \exp(\lambda_A \Pi))^2} \quad (36)$$

which provides an excellent semiquantitative fit to the experimentally observed promotional kinetics as shown in Figure 16. This simple expression predicts indeed purely electrophobic behaviour for strong adsorption of A ( $k_D = 10^{-2}$ ,  $k_A = 10^2$ ), purely electrophilic behaviour for strong adsorption of D ( $k_D = 10^2$ ,  $k_A = 10^{-2}$ ) and volcano-type behaviour for strong adsorption of A and D

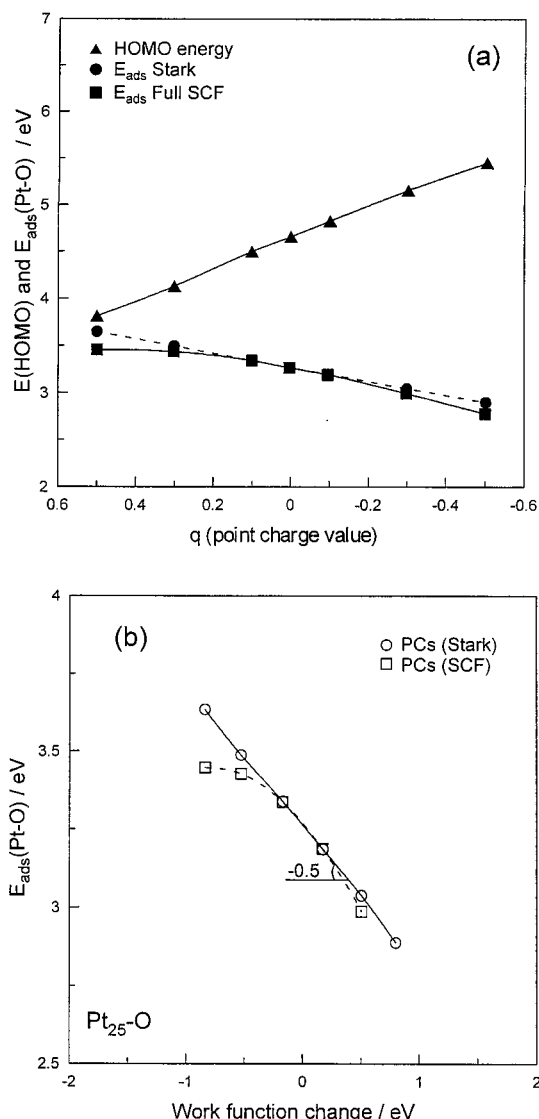


Figure 15. (a) Dependence of the position of the HOMO in  $Pt_{25}$  and of the  $Pt_{25}/O$  adsorption energy,  $E_{ads}$ , at the Stark and full self-consistent field (SCF) levels, as a function of the presence of point charge  $q$  above and below the cluster first layer. (b) Oxygen adsorption energy,  $E_{ads}$ , vs work function change, as measured by the cluster HOMO, for  $Pt_{25}/O$ . The curves refer to the cluster with point charges (PC). Both Stark and full SCF curves are shown [127]. Reprinted with permission from the American Chemical Society.

( $k_D = k_A = 10^2$ ). In the case of weak adsorption of A and D, since repulsive lateral interactions can be neglected, [2, 121] Eq. (36) is replaced by:

$$r = \frac{k_R k_A k_D p_A p_D \exp[\max(0, \lambda_D \Pi)] + [\max(0, \lambda_A \Pi)]}{(1 + k_D p_D \exp[\max(0, \lambda_D \Pi)] + k_A p_A \exp[\max(0, \lambda_A \Pi)])^2} \quad (37)$$

which also nicely predicts inverted-volcano behaviour for  $k_A = k_D = 10^{-2}$  (Fig. 16d).

The success of the model can be appreciated from Figure 17 which compares model predictions (top, Fig. 17a and b) with some truly interesting and complex experimental results (bottom, Fig. 17c and d) obtained

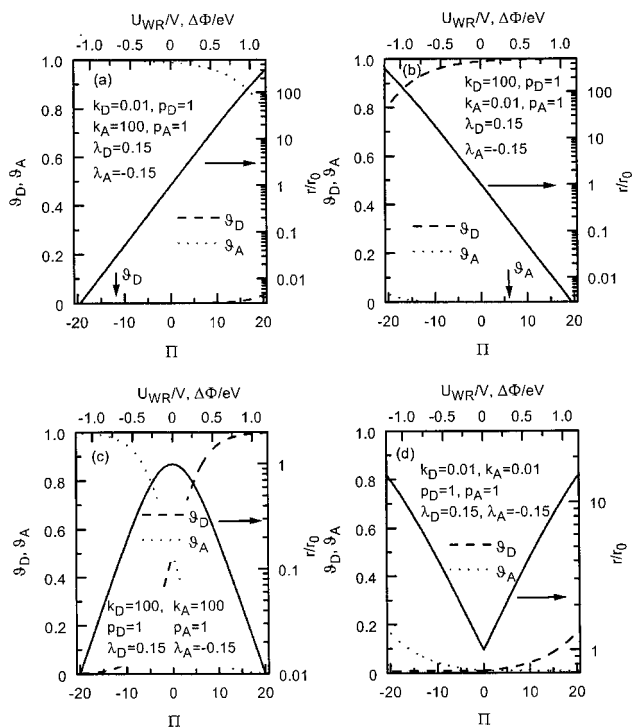


Figure 16. Model predicted electrochemical promotion behaviour: (a) electrophobic, (b) electrophilic, (c) volcano-type, (d) inverted volcano-type.

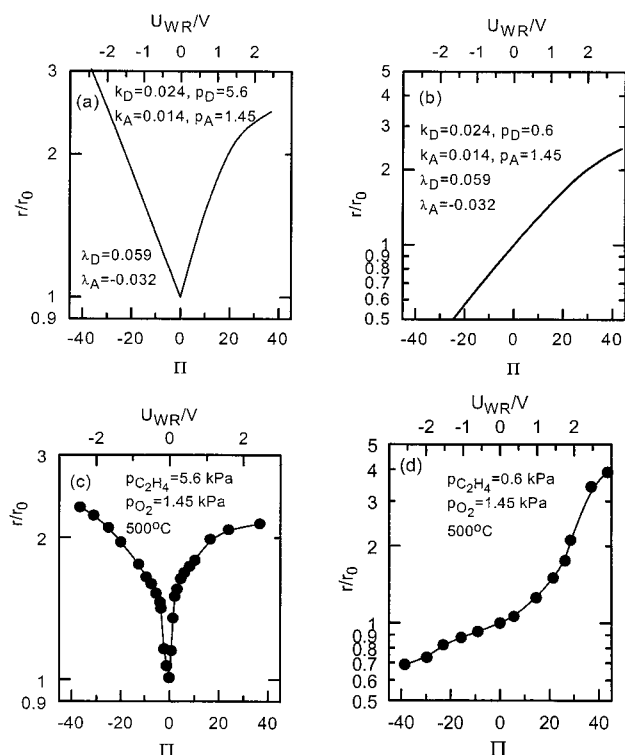


Figure 17. Experimentally observed (bottom) and model predicted (top) transition from inverted volcano to electrophobic behaviour upon increasing the  $O_2$  to ethylene (i.e. A/D) ratio by a factor of 10,  $C_2H_4$  oxidation on  $Pt/TiO_2$  [57]. Reprinted with permission from Academic Press.

during  $C_2H_4$  oxidation on  $Pt/TiO_2$  [57,122]. As shown in Figure 17c and d (bottom) the rate dependence on  $U_{WR}$  and  $[\Pi]$  shifts from inverted volcano (Fig. 17c) to purely electrophobic (Fig. 17d) as  $p_{C_2H_4}(=p_D)$  is decreased by a factor of 10 at fixed  $p_{O_2}$ . As shown in Figure 17a and b (top) the model predicts the shift in global behaviour in a truly impressive semiquantitative manner and in fact with very reasonable  $\lambda_D$  and  $\lambda_A$  values ( $\lambda_D > 0$ ,  $\lambda_A < 0$ ).

Finally the success of the model can be judged from Figures 18a and b which show the experimental and model-predicted rate dependence on  $p_{CO}$  and work function during CO oxidation on  $Pt/\beta''-Al_2O_3$  [61]. Note the transition from a classical Langmuir-Hinshelwood to a positive order rate dependence on  $p_{CO}$  with decreasing work function. Also notice that on every point of the experimental or model predicted rate dependence, the basic promotional rule:

$$\left(\frac{\partial r}{\partial \Phi}\right)_{P_A, P_D} \left(\frac{\partial r}{\partial p_D}\right)_{\Phi, P_A} > 0 \quad (38)$$

is strictly obeyed. The optimal  $\lambda_D$  and  $\lambda_A$  values are again quite reasonable ( $\lambda_D > 0$ ,  $\lambda_A < 0$ ). The large optimal  $k_A$  and  $k_D$  values ( $\sim 9$ ) are also quite reasonable as they indicate strong adsorption of both CO ( $=D$ ) and oxygen ( $=A$ ) which is the necessary and sufficient condition (Rule G3) for the appearance of volcano-type behavior.

In general Figures 16 to 18 show, beyond any reasonable doubt, that the effective double layer model of promotion, expressed mathematically by Equation (36), grasps the essence of promotional kinetics [2].

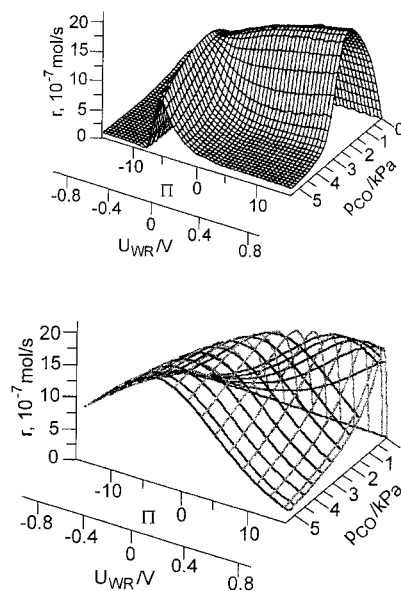


Figure 18. Experimental [61] (top) and model simulated [133] (bottom) dependence of the rate of CO oxidation on Pt deposited on  $\beta''-Al_2O_3$  as a function of  $p_{CO}$ , catalyst potential  $U_{WR}$  and dimensionless catalyst work function  $\Pi(=\Delta\Phi/k_bT)$  at  $p_{O_2}=6$  kPa.[61] Parameters used in equations (52) and (53):  $k_A=9.133$ ,  $k_D=8.715$ ,  $\lambda_A=-0.08$ ,  $\lambda_D=0.09$ ,  $\lambda_R=0$ ,  $k_R=6.19 \cdot 10^{-6}$ . Reprinted with permission from Academic Press.

## 2. THE MECHANISM OF METAL-SUPPORT INTERACTIONS

### 2.1. Self-driven NEMCA: The bridge between electrochemical promotion and metal-support interactions

Before discussing in the next section the series of experimental results which proved the functional identity of electrochemical promotion and metal-support interactions with  $O^{2-}$  conduction (YSZ) and mixed  $O^{2-}$ -electronic conducting ( $TiO_2$ ,  $CeO_2$ ) supports, it is useful to first review an experiment reported in 1993 by Cavalca, Larsen, Vayenas and Haller [130] in the course of their investigation of electrochemical promotion of methanol oxidation on Pt deposited on YSZ in a single-chamber reactor (Fig. 19). Cavalca et al. [130] noticed (as one easily observes in any electrochemical promotion study using the single-chamber design) that a *negative* potential appears ( $U_{WR} \approx -0.3$  V) between the Pt catalyst and the Ag counter and reference electrodes *under open-circuit conditions*.

This negative potential is easy to understand and is actually used nowadays in the *single chamber fuel cells* [2]: Oxygen is consumed by the catalytic reaction of  $CH_3OH$  oxidation much faster on the Pt catalyst-electrode than on the Ag counter electrode (Ag is also a catalyst for  $CH_3OH$  oxidation and partial oxidation, but much less active than Pt). Consequently the observed open-circuit potential is a Nernst potential:

$$U_{WC}^0 = (1/4e) (\mu_{O_2(Pt)} - \mu_{O_2(Ag)}) = \frac{RT}{4F} \ln \left( \alpha_{O_2(Pt)}^2 / \alpha_{O_2(Ag)}^2 \right) \quad (39)$$

where the oxygen chemical potential and activity on Pt are significantly smaller than on Ag (due to the faster catalytic reaction on Pt which forces the oxygen adsorption step to be not in equilibrium) thus  $U_{WC}^0$  is negative.

Cavalca et al. [130] utilized this self-created potential and the fact that methanol oxidation on Pt exhibits *electrophobic behaviour*, i.e. is promoted by  $O^{2-}$  supply to the catalyst, to induce NEMCA (electrochemical promotion) on Pt *without an external power source (galvanostat or potentiostat) by just short-circuiting the catalyst and the counter electrode* (Fig. 19a).

What is the mechanism of electrochemical promotion under these short-circuit conditions? It is very simple as shown in Figure 19. Upon short circuiting, the Fermi levels in the Pt catalyst and Ag counter electrode become equal and  $O^{2-}$  are being continuously supplied to the Pt catalyst, inducing NEMCA and attempting to establish there an oxygen chemical potential  $\mu_{O_2(Pt)}$  equal to that on Ag. Due to the fast catalytic reaction on Pt this is not possible and thus the  $O^{2-}$  flux to the Pt catalyst continuous *ad infinitum*. The spent  $O^{2-}$  are continuously replenished by gaseous  $O_2$  at the Ag counter electrode. This is a *self-driven NEMCA system*, suitable for promoting *any electrophobic reaction*.

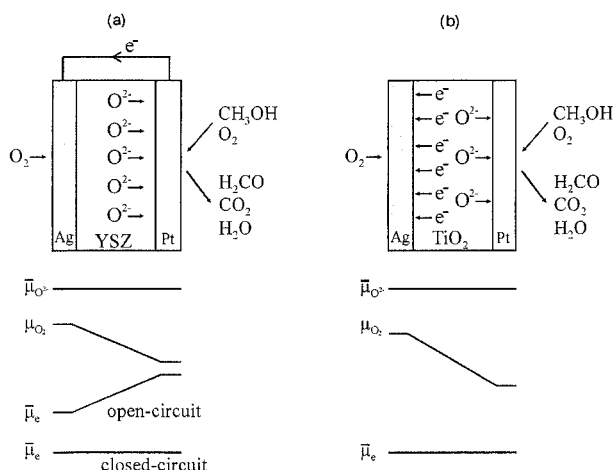


Figure 19. Self-driven electrochemical promotion of  $CH_3OH$  oxidation on Pt using  $O^{2-}$  conductor (YSZ) with external catalyst-counter electrode short-circuiting (a) and a mixed ionic ( $O^{2-}$ )-electronic conductor ( $TiO_2$ ) with internal short-circuiting.

To compensate the  $O^{2-}$  flux and close the circuit there is an electric current flowing through the short-circuiting wire (Fig. 19a). Now let us imagine that YSZ is replaced by  $TiO_2$  which has both ionic ( $O^{2-}$ ) and electronic conductivity (Fig. 19b). In this case the need for the short-circuiting wire is eliminated as the electronic current can flow in the  $TiO_2$  pellet itself. Under these conditions there is no net current flowing in the  $TiO_2$  pellet but the Pt catalyst is electrochemically promoted. This is again a *self-driven NEMCA system suitable for any electrophobic reaction* and having no net current flowing anywhere in it (the  $O^{2-}$  current in the  $TiO_2$  is equal and opposite to the electronic current).

The similarity with  $TiO_2$ -supported dispersed Pt catalyst is obvious. For if  $O^{2-}$  backspillover can take place over *mm distances* on the porous Pt films used for electrochemical promotion studies with YSZ and  $TiO_2$  (as proven conclusively by XPS and several other techniques[134]) it can certainly take place over *nm distances* on the supported Pt nanoparticles of commercial highly dispersed YSZ and  $TiO_2$  supported catalysts.

Do we really need a Ag counter electrode in this self-driven NEMCA (or metal-support interaction promoted) system? The answer is no, for two reasons:

1. With the usual size distribution of nanoparticles in a commercial  $ZrO_2$ - or  $TiO_2$ - or  $CeO_2$ - supported noble metal catalyst, each two dissimilar size crystallites create a small local galvanic cell able to electrochemically promote one of the two nanoparticles.

2. In mixed conducting supports ( $TiO_2$ ,  $CeO_2$ ) but also on doped  $ZrO_2$  direct replenishment of  $O^{2-}$  by gaseous  $O_2$  is rather efficient:



Thus on the basis of the experiments of Cavalca et al. [130], in conjunction with the plethora of surface

spectroscopic investigations of NEMCA [2,134], it is reasonable to anticipate that the mechanism of metal–support interaction induced promotion of catalytic oxidations is the same with the mechanism of self-driven electrochemical promotion systems: *self-induced migration of promoting  $O^{2-}$  species on the nanoparticle catalyst surface* [135].

## 2.2. Confirmation of the self-driven NEMCA metal–support interaction mechanism

Three independent systems were used by Nicole, Tsiplakides, Pliangos, Verykios, Comninellis and Vayenas [135] to show the mechanistic equivalence of NEMCA and metal–support interactions (Fig. 20).

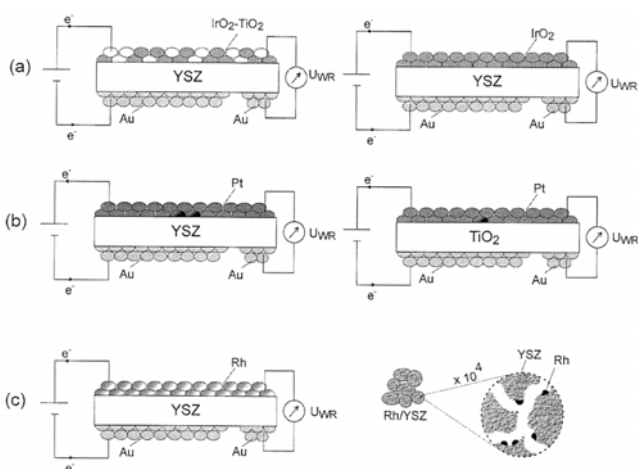


Figure 20. Schematic of the experimental setup used (a) to induce electrochemical promotion (via YSZ) on IrO<sub>2</sub> and IrO<sub>2</sub>-TiO<sub>2</sub> porous catalyst films (b) to compare the electrochemical promotion induced on Pt via YSZ and via TiO<sub>2</sub> and (c) to compare the electrochemical promotion behaviour induced by varying  $U_{WR}$  on a Rh porous catalyst film (left) and on a fully dispersed Rh catalyst supported on porous (80 m<sup>2</sup>/g) YSZ support.[135]

Here we discuss the results obtained for the model reaction of C<sub>2</sub>H<sub>4</sub> oxidation on IrO<sub>2</sub>, Pt and Rh but similar conclusions are reached when using other model reactions such as CO oxidation or NO reduction by CO [135].

The three systems shown in Figure 20 were used to compare:

a) The open-circuit and NEMCA induced catalytic activity of IrO<sub>2</sub> (which is a metal-type conducting metal oxide [136]) and of mixed IrO<sub>2</sub>-TiO<sub>2</sub> catalysts consisting of micro- and nanoparticles of IrO<sub>2</sub> (active phase) and TiO<sub>2</sub> (inert support) in intimate contact (Fig. 20a) [137].

b) The open-circuit and NEMCA induced catalytic activity of Pt films deposited on YSZ [19] and on TiO<sub>2</sub> [135]. In this case XPS was also used in vacuum [80,135] to quantify the coverage of the backspillover O<sup>2-</sup> species on the Pt surface (Fig. 20b).

c) The catalytic rate enhancement induced on porous Rh films via electrochemical promotion with YSZ (Fig. 20c, left [33]) and that induced on dispersed Rh nanoparticles upon varying the porous, high surface area (~100 m<sup>2</sup>/g) catalyst support (TiO<sub>2</sub>, SiO<sub>2</sub>,  $\gamma$ -Al<sub>2</sub>O<sub>3</sub>, YSZ and TiO<sub>2</sub> doped with 4 mol% WO<sub>3</sub>) [138]. In all five cases the Rh metal loading was 0.5 wt% [138].

In view of the title of this section the reader can anticipate and predict the results of these key experiments [135]:

(a) There is similar, roughly 12-fold, maximum rate enhancement induced on the IrO<sub>2</sub> catalyst via NEMCA ( $p \approx 12$ , pure IrO<sub>2</sub>, Fig. 21) and via metal–support interactions of IrO<sub>2</sub> with TiO<sub>2</sub> ( $p_{MSI} \approx 13$ ,  $X_{IrO_2} \approx 0.5$ , (Fig. 21). The parameter  $p_{MSI}$  is defined from:

$$p_{MSI} = r/r_u \quad (13)$$

where  $r_u$  is the (unpromoted) catalytic rate per unit mass of the active catalyst and  $r$  is the same (promoted) catalytic rate, enhanced due to the metal–support interaction.

Moreover, as also shown in Fig. 21, there is practically *no electrochemical promotion* ( $p < 1.5$ ) of the mixed IrO<sub>2</sub>-TiO<sub>2</sub> catalyst. It is thus clear that IrO<sub>2</sub> in the IrO<sub>2</sub>-TiO<sub>2</sub> catalyst is already in an electrochemically promoted state. It thus becomes apparent that TiO<sub>2</sub> is constantly supplying O<sup>2-</sup> to the IrO<sub>2</sub> surface. This ingenious experiment is due to Nicole and Comninellis [137]. Note that pure TiO<sub>2</sub> ( $X_{IrO_2} = 0$ ) is always inactive (Fig. 21).

(b) There is similar transient and steady-state electrochemical promotion behaviour of Pt on YSZ and

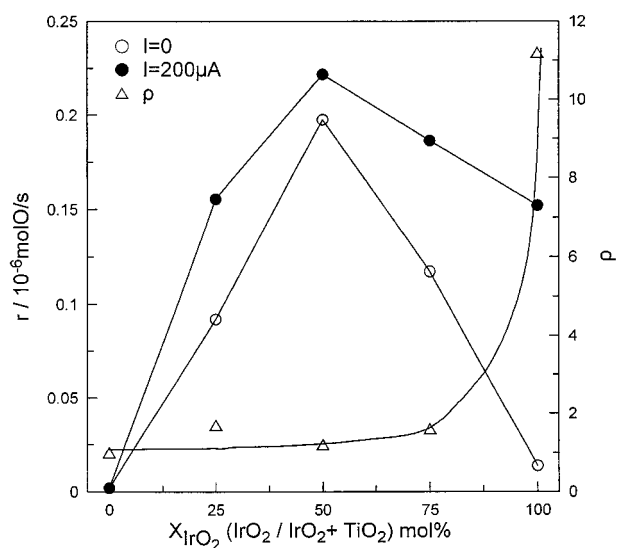


Figure 21. Effect of the mole fraction,  $X_{IrO_2}$ , of IrO<sub>2</sub> in the IrO<sub>2</sub>-TiO<sub>2</sub> catalyst film on the rate of C<sub>2</sub>H<sub>4</sub> oxidation under open-circuit conditions (open circles) and under electrochemical promotion conditions (filled circles) via application of  $I=200 \mu\text{A}$ ;  $T=380^\circ\text{C}$ ,  $p_{C_2H_4}=0.15 \text{ kPa}$ ,  $p_{O_2}=20 \text{ kPa}$ . Triangles indicate the corresponding electrochemical promotion rate enhancement ratio  $p$  values [135,137].

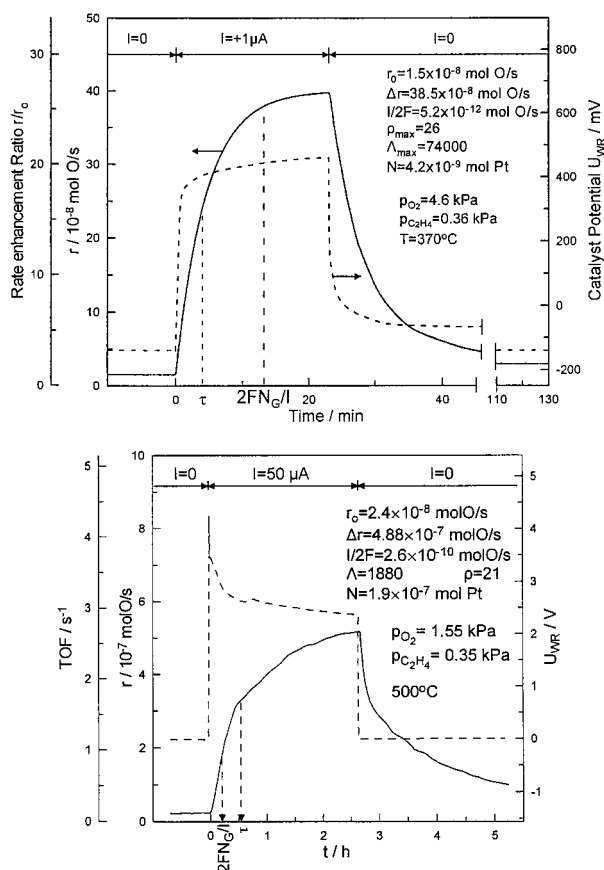


Figure 22. Galvanostatic catalytic rate transients showing the equivalence of electrochemical promotion when using YSZ[19] (a) or TiO<sub>2</sub> [57] (b) as the Pt metal film support. See text for discussion [135]. Reprinted with permission from Academic Press.

Pt on TiO<sub>2</sub> (Figs. 22a and 22b) and similar O<sup>2-</sup> backspillover mechanism of Pt on YSZ and of Pt on TiO<sub>2</sub> as manifest by XPS (Fig. 23).

In particular:

In both cases imposition of a positive current  $I$  (with a concomitant rate,  $I/2F$ , of supply of O<sup>2-</sup> to the catalyst for the case of Pt/YSZ and an also concomitant increase in catalyst potential  $U_{WR}$ ) causes a pronounced, 25 fold in Fig. 22a, 22 fold in Fig. 22b, increase in catalytic rate ( $\rho=26$  and  $\rho=23$  respectively).

The Faradaic efficiency  $\Lambda$  is  $74 \cdot 10^3$  in Fig. 22a (YSZ) and  $1.88 \cdot 10^3$  in Fig. 22b (TiO<sub>2</sub>) suggesting that only a fraction  $f$  ( $\approx 2.5\%$ ) of the current  $I$  in TiO<sub>2</sub> is anionic (O<sup>2-</sup>), the rest being electronic, in good agreement with the literature [135]. This is nicely confirmed by comparing the time,  $\tau$ , required for the rate increase to reach 63% of its steady state value with the parameter  $2FN_G/I$  (Fig. 22). In the case of YSZ,  $\tau$  is shorter than  $2FN_G/I$  while in the case of TiO<sub>2</sub>  $\tau$  is longer than  $2FN_G/I$ , again suggesting that only a fraction of the current  $I$  in TiO<sub>2</sub> is ionic. By comparing the ratio  $\tau/(2FN_G/I)$  in both cases one may conclude that  $f \approx 0.05$ , in qualitative agreement with the value estimated from the Faradaic efficiency,  $\Lambda$ , values.

(c) There is similar electrochemical promotion behaviour of Rh films on YSZ and similar metal-support

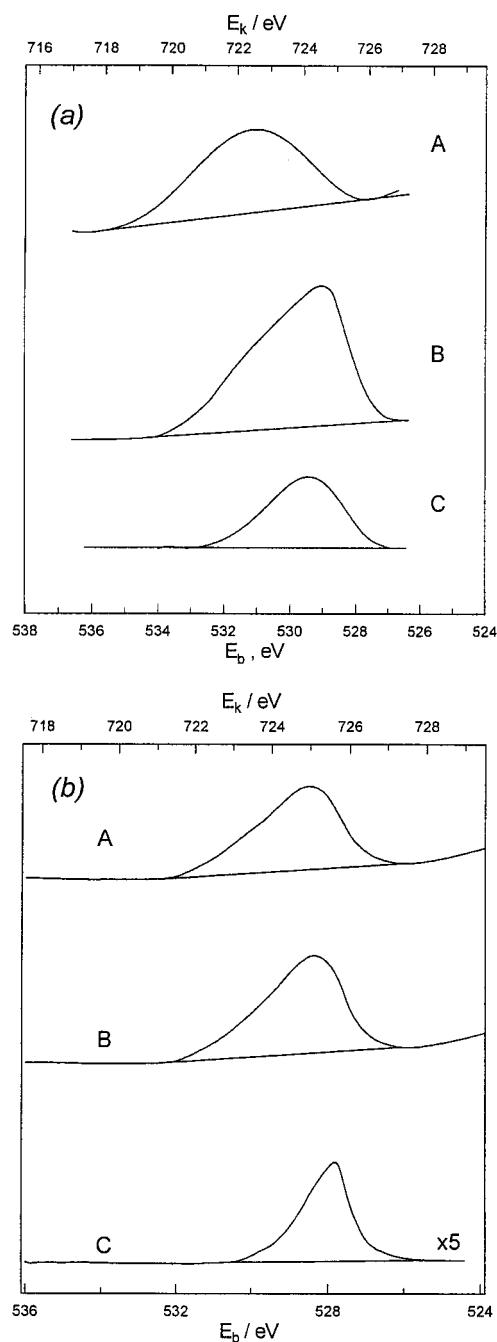


Figure 23. XPS confirmation of O $\delta^-$  backspillover as the mechanism of electrochemical promotion on Pt films deposited on YSZ (a) and on TiO<sub>2</sub> (b). Adapted from refs. [57,80]. In both cases A is the open-circuit O1s spectrum, B is the O1s spectrum under anodic ( $I > 0$ ,  $\Delta U_{WR} > 0$ ) polarization and C is the difference spectrum [57,80,135]. Reprinted with permission from the American Chemical Society (a, ref. 80) and from Academic Press (b, 57).

interaction-induced behaviour of dispersed Rh on different supports for the model reaction of C<sub>2</sub>H<sub>4</sub> oxidation on Pt. (Fig. 24). In particular there are very similar  $\rho$  values ( $\rho \approx \rho_{MSI} \approx 120$ ) upon increasing the potential and work function of the Rh film or upon increasing the work function (or absolute potential) of the support of the dispersed Rh catalyst (Figure 24).

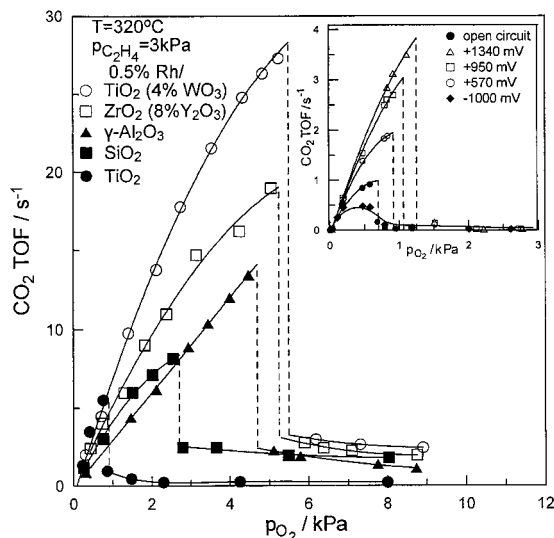


Figure 24. Effect of  $p_{O_2}$  on the rate (TOF) of  $C_2H_4$  oxidation on Rh supported on five supports of increasing  $\Phi$ . Catalyst loading 0.5wt% [135,140]. Inset: Electrochemical promotion of a Rh catalyst film deposited on YSZ: Effect of potentiostatically imposed catalyst potential  $U_{WR}$  on the rate and TOF dependence on  $p_{O_2}$  at fixed  $p_{C_2H_4}$  [135,140]. Reprinted with permission from Elsevier Science (ref. 135) and Academic Press (ref. 140).

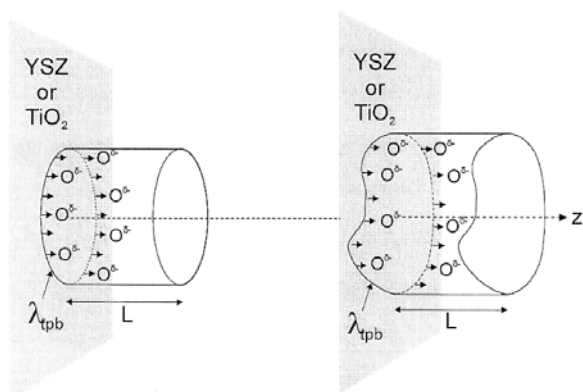
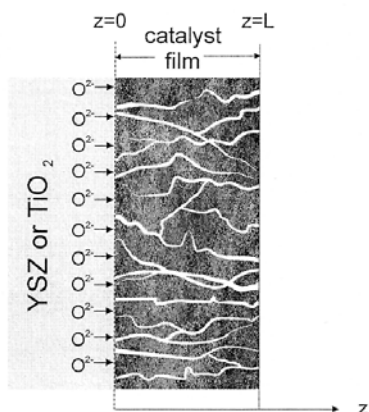


Figure 25. Schematic of an electrochemically promoted metal catalyst film supported on a  $O^{2-}$  conductor (top) [139] and schematic of cylindrical or, more generally, fixed cross-section nanoparticles deposited on an  $O^{2-}$  conducting support (bottom). [139]

## 2.2.1. Mathematical modeling and range of operability of electrochemical promotion and of metal-support interactions

In view of the functional similarity of electrochemical promotion and metal support interactions, a mathematical promoter consumption–promoter diffusion model has been developed recently [139] in order to identify the dimensionless groups which governs both phenomena and quantify their limits of applicability.

The model geometries are shown in Fig. 25 and the basic dimensionless promoter ( $O^{2-}$ ) reaction–diffusion equation, governing both phenomena, is:

$$\frac{d^2\theta_i}{d\xi^2} - \Phi_P^2\theta_i = 0 \quad (41)$$

with boundary conditions:

$$\xi = 0; \frac{d\theta_i}{d\xi} = -J\Phi_P^2(1 - \theta_i) \quad (42)$$

$$\xi = 1; d\theta/d\xi = 0 \quad (43)$$

where  $\xi$  is the dimensionless distance across the electrochemically promoted catalyst film or nanoparticle,  $\theta_i$  is the coverage of the backspillover  $O^{2-}$  species, and  $\Phi_P$  and  $J$  are the promotional Thiele modulus and dimensionless current, respectively, defined from:

$$\Phi_P = L\sqrt{k/D_s} \quad (44)$$

$$J = l/(2FkC_{i,max}A_c) \text{ for electrochemical promotion} \quad (45)$$

$$J = (r/A_c)/(\Lambda kC_{i,max}) \text{ for MSI} \quad (46)$$

Here  $L$  is the catalyst film thickness or nanoparticle size,  $k$  is the rate constant for depletion (reaction or desorption) of the promoting  $O^{2-}$  species,  $C_{i,max}$  is its maximum possible surface concentration on the catalyst or nanoparticle surface,  $A_c$  is the metal/gas interface area of the film or nanoparticle,  $r$  is the promoted catalytic rate and  $\Lambda$  is the Faradaic efficiency of the catalytic reaction which is being promoted.

Solution of Equation with boundary conditions and leads to the following expressions for the rate enhancement ratio  $\rho$  in terms of the dimensionless dipole moment,  $\Pi$ , of the promoting species:

$$\rho = \exp(\Pi\eta_P) \quad (47)$$

$$\Pi = \frac{\alpha e N_M P_i}{\epsilon_0 k_b T} \quad (48)$$

where  $\eta_P$  is the promotional effectiveness factor defined from:

$$\eta_P = \int_0^1 \theta_i(\xi) d\xi \quad (49)$$

and computed from:

$$1/\eta_P = 1/J + \Phi_P/\tanh\Phi_P \quad (50)$$

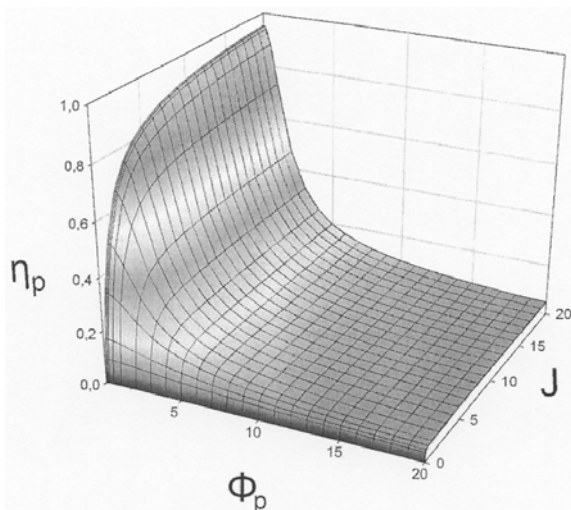


Figure 26. Dependence of promotional effectiveness factor,  $\eta_p$ , on Thiele modulus  $\Phi_p$  and dimensionless current  $J$  [139].

In order to have significant electrochemical promotion or metal–support interaction promotion of a catalytic reaction,  $\eta_p$  must be at least 0.2. Equation and the corresponding figure 26 shows the range of  $\Phi_p$  and  $J$  values which allow for this to happen: The Thiele modulus  $\Phi_p$  must be smaller than five. This means small film thickness or catalyst particle size, small kinetic constant  $k$  for promoter destruction and finite surface diffusivity,  $D_s$ , of the promoter. Also the dimensionless current  $J$  must be larger than two and this again dictates a small  $k$  value for promoter destruction, a finite current for electrochemical promotion and a fast catalytic rate,  $r$ , for metal–support interactions.

### 3. INTERRELATION OF PROMOTION, ELECTROCHEMICAL PROMOTION AND METAL–SUPPORT INTERACTIONS: THE DOUBLE LAYER MODEL OF CATALYSIS

Promotion, electrochemical promotion and metal–support interactions are three, at a first glance, independent phenomena which can affect catalyst activity and selectivity in a dramatic manner. However, as recently discovered, promotion, electrochemical promotion and metal–support interactions on ion–conducting and mixed–conducting supports are three different facets of the same phenomenon. They are all three linked via the phenomenon of spillover–backspillover. And they are all three due to the same underlying cause: The interaction of adsorbed reactants and intermediates with an effective double layer formed by promoting species at the metal/gas interface (Fig. 27).

For time scales shorter than that of a catalytic turnover (typically  $10^{-2}$  to  $10^2$  s) the three phenomena are indistinguishable. Looking at the Na–promoted Pt surface in Fig. 28 and imagining that CO oxidation is taking place on that surface, there is no way to distinguish if this is a classically promoted surface where Na has been added from the gas phase, or an

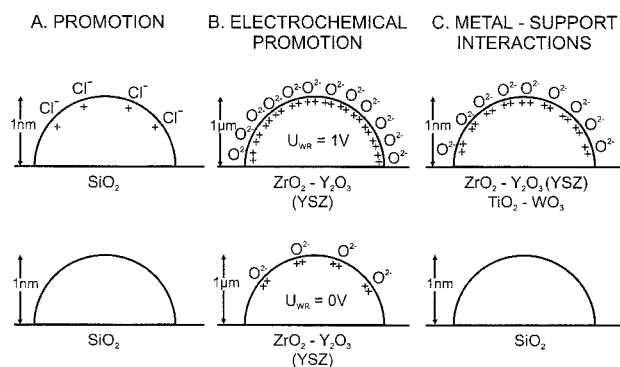


Figure 27. Schematic of the promotional mechanism for electrophobic reactions: A: via electronegative promoter addition of long lifetime (classical promotion), B: via potential- or current controlled  $O^{2-}$  backspillover (electrochemical promotion), C: via self-driven  $O^{2-}$  backspillover (metal–support interactions).

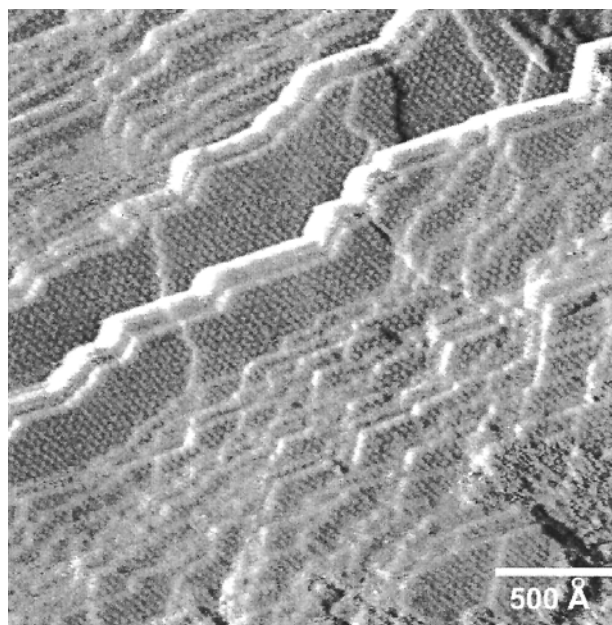


Figure 28. STM image (unfiltered) of a Pt single crystal surface consisting mainly of Pt(111) terraces and covered by a Pt(111)–(12x12)–Na adlattice formed via electrochemical  $Na^+$  supply (from a  $\beta''$ - $Al_2O_3$   $Na^+$  conductor interfaced with the Pt single crystal) on a Pt(111)–(2x2)–O adlattice. Each sphere on the image corresponds to a Na atom. [2, 129, 148]

electrochemically promoted one where Na originated from  $\beta''$ - $Al_2O_3$  interfaced with the Pt crystal, or finally if it is the surface of a larger crystallite deposited on a porous  $\beta''$ - $Al_2O_3$  carrier where Na has spontaneously migrated on the Pt surface (metal–support interaction). The oxidation of CO will be equally promoted in all three cases.

Similar would be the situation on a Pt surface decorated with  $O^{2-}$ , the only difference being the experimental difficulty of introducing  $O^{2-}$  with classical promotion and its short lifetime on the catalyst surface, only  $\Delta$  times longer than the catalytic turnover.

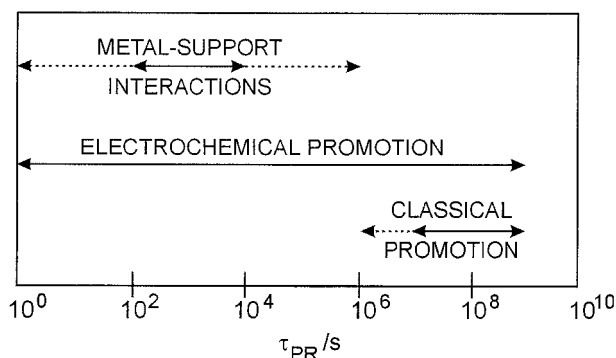


Figure 29. Operational range of classical promotion, electrochemical promotion and metal-support interactions in terms of the promoter lifetime on the catalyst surface.

Consequently the proven functional identity of classical promotion, electrochemical promotion and metal-support interactions should not lead the reader to pessimistic conclusions regarding the practical usefulness of electrochemical promotion. Operational differences exist between the three phenomena and it is very difficult to imagine how one can use metal-support interactions with conventional supports to promote an electrophilic reaction or how one can use classical promotion to generate the strongest electronegative promoter,  $O^{2-}$ , on a catalyst surface. Furthermore there is no reason to expect that a metal-support-interaction-promoted catalyst is at its "best" electrochemically promoted state. Thus the experimental problem of inducing electrochemical promotion on fully-dispersed catalysts remains an important one [2].

Having discussed the functional equivalence of classical promotion, electrochemical promotion and metal-support interactions on  $O^{2-}$ -conducting and mixed electronic-ionic conducting supports, it is useful to also address and systematize their operational differences. This is attempted in Figure 29: The main operational difference is the promoter lifetime,  $\tau_{PR}$ , on the catalyst surface (Fig. 29).

For any practical classical promotion application in a fixed bed catalytic reactor,  $\tau_{PR}$  must be longer than a year ( $\sim 3 \cdot 10^7$  s). But even for lab scale classical promotion experiments  $\tau_{PR}$  values in excess of  $10^6$  s are required (Fig. 29). On the other hand electrochemical promotion is not subject to any such restrictions regarding  $\tau_{PR}$  (Fig. 29). Thus when using  $O^{2-}$  conductors or  $H^+$  conductors,  $\tau_{PR}$  is  $10^2$ – $10^4$  s, but when using  $Na^+$  conductors  $\tau_{PR}$  can be well in excess of  $10^7$  s at low  $T$ , but also in the range  $10^4$ – $10^6$  s for higher  $T$ .

This is an important operational advantage of electrochemical promotion: It permits the use of a wide variety of sacrificial promoters (e.g.  $O^{2-}$ ,  $H^+$ ) which have too short life times for classical promotion applications.

#### ACKNOWLEDGEMENT

We thank BASF for financial support.

#### REFERENCES

- [1] M. Kiskinova, Poisoning and Promotion in Catalysis based on Surface Science Concepts and Experiments, in *Stud. Surf. Sci. Catal.* **70**, Elsevier, Amsterdam (1992).
- [2] C.G. Vayenas, S. Bebelis, C. Pliangos, S. Brosda, and D. Tsiplakides, *Electrochemical Activation of Catalysis: Promotion, Electrochemical Promotion and Metal-Support Interactions*, Kluwer/Plenum Press, New York (2002).
- [3] C.G. Vayenas, M.M. Jaksic, S. Bebelis, and S.G. Neophytides, *The Electrochemical Activation of Catalysis*, in *Modern Aspects of Electrochemistry*, J.O.M. Bockris, B.E. Conway, and R.E. White, eds., Kluwer Academic/Plenum Publishers, New York (1996), pp. 57–202.
- [4] E. Lamy-Pitara, L. Bencharif, and J. Barbier, *Appl. Catal.* **18** (1985) 117–131.
- [5] M. Stoukides, and C.G. Vayenas, *J. Catal.* **70** (1981) 137–146.
- [6] C.G. Vayenas, S. Bebelis, and S. Neophytides, *J. Phys. Chem.* **92** (1988) 5083–5085.
- [7] C.G. Vayenas, S. Bebelis, and S. Ladas, *Nature* **343** (1990) 625–627.
- [8] J. Pritchard, *Nature* **343** (1990) 592.
- [9] H. Baltruschat, N.A. Anastasijevic, M. Beltowska-Brzezinska, G. Hambitzer, and J. Heitbaum, *Ber. Buns. Phys. Chem.* **94** (1990) 996–1000.
- [10] T.I. Politova, V.A. Sobyenin, and V.D. Belyaev, *Reaction Kinetics and Catalysis Letters* **41**(2) (1990) 321–326.
- [11] E. Varkaraki, J. Nicole, E. Plattner, C. Comminellis, and C.G. Vayenas, *J. Appl. Electrochem.* **25** (1995) 978–981.
- [12] I. Harkness, and R.M. Lambert, *J. Catal.* **152** (1995) 211–214.
- [13] C.A. Cavalca, and G.L. Haller, *J. Catal.* **177** (1998) 389–395.
- [14] L. Ploense, M. Salazar, B. Gurau, and E.S. Smotkin, *JACS* **119** (1997) 11550–11551.
- [15] J. Poppe, S. Voelkening, A. Schaak, E. Schuetz, J. Janek, and R. Imbuhl, *Phys. Chem. Chem. Phys.* **1** (1999) 5241–5249.
- [16] J.K. Hong, I.-H. Oh, S.-A. Hong, and W.Y. Lee, *J. Catal.* **163** (1996) 95–105.
- [17] D.A. Emery, P.H. Middleton, and I.S. Metcalfe, *Surf. Sci.* **405** (1998) 308–315.
- [18] J.O.M. Bockris, and Z.S. Minevski, *Electrochim. Acta* **39** (11/12) (1994) 1471–1479.
- [19] S. Bebelis, and C.G. Vayenas, *J. Catal.* **118** (1989) 125–146.
- [20] C.G. Vayenas, S. Bebelis, I.V. Yentekakis, and H.-G. Lintz, *Catalysis Today* **11**(3) (1992) 303–442.
- [21] C.G. Vayenas, and S. Bebelis, *Catalysis Today* **51**(1999) 581–594.
- [22] C.G. Vayenas, and S. Neophytides, *Electrochemical Activation of Catalysis: In situ controlled promotion of catalyst surfaces*, in *Catalysis-Special periodical Report*, Royal Society of Chemistry, Cambridge (1996), pp. 199–253.
- [23] C.G. Vayenas, and I.V. Yentekakis, *Electrochemical Modification of Catalytic Activity*, in *Handbook of Catalysis*, G. Ertl, H. Knötzinger, and J. Weitcamp, eds., VCH Publishers, Weinheim (1997), pp. 1310–1338.
- [24] S. Bebelis, M. Makri, A. Buekenhoudt, J. Luyten, S. Brosda, P. Petrolekas, C. Pliangos, and C.G. Vayenas, *Solid State Ionics* **129**, 33–46 (2000).
- [25] A. Kaloyannis, and C.G. Vayenas, *J. Catal.* **171** (1997) 148–159.
- [26] P. Tsiakaras, and C.G. Vayenas, *J. Catal.* **140** (1993) 53–70.
- [27] C.G. Vayenas, S. Bebelis, I.V. Yentekakis, P. Tsiakaras, and H. Karasali, *Platinum Metals Review* **34** (3) (1990) 122–130.
- [28] I.V. Yentekakis, and C.G. Vayenas, *J. Catal.* **111** (1988) 170–188.

- [29] H. Karasali, and C.G. Vayenas, *Materials Science Forum* **76** (1991) 171–174.
- [30] C.G. Vayenas, and S. Neophytides, *J. Catal.* **127** (1991) 645–664.
- [31] A. Kaloyannis, and C.G. Vayenas, *J. Catal.* **182** (1999) 37–47.
- [32] M. Marwood, A. Kaloyannis, and C.G. Vayenas, *Ionics* **2** (1996) 302–311.
- [33] C. Pliangos, I.V. Yentekakis, X.E. Verykios, and C.G. Vayenas, *J. Catal.* **154** (1995) 124–136.
- [34] C. Pliangos, C. Raptis, T. Badas, and C.G. Vayenas, *Solid State Ionics* **136/137** (2000) 767–773.
- [35] C. Pliangos, C. Raptis, T. Badas, and C.G. Vayenas, *Ionics* **6** (2000) 119–126.
- [36] A.D. Frantzis, S. Bebelis, and C.G. Vayenas, *Solid State Ionics* **136–137** (2000) 863–872.
- [37] K. Yiokari, and S. Bebelis, *J. Appl. Electrochem.* **30** (2000) 1277–1283.
- [38] H. Alqahtany, P.H. Chiang, P. Eng, M. Stoukides, and A.R. Robbat, *Catal. Lett.* **13** (1992) 289–296.
- [39] A. Giannikos, A.D. Frantzis, C. Pliangos, S. Bebelis, and C.G. Vayenas, *Ionics* **4** (1998) 53–60.
- [40] M. Marwood, and C.G. Vayenas, *J. Catal.* **170** (1997) 275–284.
- [41] G.L. Haller, and S. Kim ACS Petroleum Division Preprints, Symposium in Catalytic Combustion in 213th National ACS Meeting, (1997, April 13–17) San Francisco, CA, pp. 155–158.
- [42] S. Bebelis, and C.G. Vayenas, *J. Catal.* **138** (1992) 570–587.
- [43] S. Bebelis, and C.G. Vayenas, *J. Catal.* **138** (1992) 588–610.
- [44] C. Karavasilis, S. Bebelis, and C.G. Vayenas, *J. Catal.* **160** (1996) 190–204.
- [45] M. Stoukides, and C.G. Vayenas, *J. Electrochem. Soc.* **131** (4), (1984) 839–845.
- [46] P. Tsiakaras, and C.G. Vayenas, *J. Catal.* **144** (1993) 333–347.
- [47] C. Karavasilis, S. Bebelis, and C.G. Vayenas, *Materials Science Forum* **76** (1991) 175–178.
- [48] S. Neophytides, and C.G. Vayenas, *J. Catal.* **118** (1989) 147–163.
- [49] O.A. Marina, and V.A. Sobyenin, *Catal. Lett.* **13** (1992) 61–70.
- [50] O.A. Marina, V.A. Sobyenin, V.D. Belyaev, and V.N. Parnon, *Catalysis Today* **13** (1992) 567–570.
- [51] T.I. Politova, G.G. Gal'vita, V.D. Belyaev, and V.A. Sobyenin, *Catal. Lett.* **44** (1997) 75–81.
- [52] I.V. Yentekakis, Y. Jiang, S. Neophytides, S. Bebelis, and C.G. Vayenas, *Ionics* **1** (1995) 491–498.
- [53] O.A. Marina, V.A. Sobyenin, V.D. Belyaev, and V.N. Parnon, The effect of electrochemical pumping of oxygen on catalytic behaviour of metal electrodes in methane oxidation, in *New Aspects of Spillover Effect in Catalysis for Development of Highly Active Catalysts*, Stud. Surf. Sci. Catal., T. Inui et al., eds., Elsevier Science Publishers B.V. (1993), pp. 337–340.
- [54] D. Tsiplakides, J. Nicole, C.G. Vayenas, and C. Comninellis, *J. Electrochem. Soc.* **145** (3) (1998) 905–908.
- [55] S. Wodiunig, and C. Comninellis, *Journal of the European Ceramic Society* **19** (1999) 931–934.
- [56] I.V. Yentekakis, and C.G. Vayenas, *J. Catal.* **149** (1994) 238–242.
- [57] C. Pliangos, I.V. Yentekakis, S. Ladas, and C.G. Vayenas, *J. Catal.* **159** (1996) 189–203.
- [58] P.D. Petrolekas, S. Balomenou, and C.G. Vayenas, *J. Electrochem. Soc.* **145** (4), (1998) 1202–1206.
- [59] P. Beatrice, C. Pliangos, W.L. Worrell, and C.G. Vayenas, *Solid State Ionics* **136–137** (2000) 833–837.
- [60] C.G. Vayenas, S. Bebelis, and S. Despotopoulou, *J. Catal.* **128** (1991) 415–435.
- [61] I.V. Yentekakis, G. Moggridge, C.G. Vayenas, and R.M. Lambert, *J. Catal.* **146** (1994) 292–305.
- [62] C.A. Cavalca, PhD Thesis, Yale University (1995).
- [63] S. Tracey, A. Palermo, J.P.H. Vazquez, and R.M. Lambert, *J. Catal.* **179** (1998) 231–240.
- [64] A. Palermo, R.M. Lambert, I.R. Harkness, I.V. Yentekakis, O. Marina, and C.G. Vayenas, *J. Catal.* **161** (1996) 471–479.
- [65] A. Palermo, M.S. Tikhov, N.C. Filkin, R.M. Lambert, I.V. Yentekakis, and C.G. Vayenas, *Ionics* **1** (1995) 366–372.
- [66] A. Palermo, M.S. Tikhov, N.C. Filkin, R.M. Lambert, I.V. Yentekakis, and C.G. Vayenas, *Stud. Surf. Sci. Catal.* **101** (1996) 513–522.
- [67] R.M. Lambert, M. Tikhov, A. Palermo, I.V. Yentekakis, and C.G. Vayenas, *Ionics* **1** (1995) 366–376.
- [68] O.A. Marina, I.V. Yentekakis, C.G. Vayenas, A. Palermo, and R.M. Lambert, *J. Catal.* **166** (1997) 218–228.
- [69] A. Giannikos, P. Petrolekas, C. Pliangos, A. Frenzel, C.G. Vayenas, and H. Putter, *Ionics* **4** (1998) 161–169.
- [70] C. Karavasilis, S. Bebelis, and C.G. Vayenas, *J. Catal.* **160** (1996) 205–213.
- [71] P.D. Petrolekas, S. Brosda, and C.G. Vayenas, *J. Electrochem. Soc.* **145** (5), (1998) 1469–1477.
- [72] G. Pitselis, P. Petrolekas, and C.G. Vayenas, *Ionics* **3** (1997) 110–117.
- [73] M. Makri, A. Buekenhoudt, J. Luyten, and C.G. Vayenas, *Ionics* **2** (1996) 282–288.
- [74] C.G. Yiokari, G.E. Pitselis, D.G. Polydoros, A.D. Katsaounis, and C.G. Vayenas, *J. Phys. Chem.* **104** (2000) 10600–10602.
- [75] P.H. Chiang, D. Eng, and M. Stoukides, *J. Catal.* **139** (1993) 683–687.
- [76] D. Tsiplakides, S. Neophytides, O. Enea, M.M. Jaksic, and C.G. Vayenas, *J. Electrochem. Soc.* **144** (6), (1997) 2072–2088.
- [77] S. Neophytides, D. Tsiplakides, P. Stonehart, M. Jaksic, and C.G. Vayenas, *Nature* **370** (1994) 292–294.
- [78] S. Neophytides, D. Tsiplakides, P. Stonehart, M.M. Jaksic, and C.G. Vayenas, *J. Phys. Chem.* **100** (1996) 14803–14814.
- [79] I.M. Petrushina, V.A. Bandur, F. Cappelin, and N.J. Bjerrum, *J. Electrochem. Soc.* **147**(8) (2000) 3010–3013.
- [80] S. Ladas, S. Kennou, S. Bebelis, and C.G. Vayenas, *J. Phys. Chem.* **97** (1993) 8845–8847.
- [81] R.M. Lambert, F. Williams, A. Palermo, and M.S. Tikhov, *Topics in Catalysis* **13**, 91–98 (2000).
- [82] W. Zipprich, H.-D. Wiemhöfer, U. Vöhrer, and W. Göppel, *Ber. Buns. Phys. Chem.* **99**, 1406–1413 (1995).
- [83] S.G. Neophytides, and C.G. Vayenas, *J. Phys. Chem.* **99** (1995) 17063–17067.
- [84] J. Poppe, A. Schaak, J. Janek, and R. Imbihl, *Ber. Buns. Phys. Chem.* **102** (1998) 1019–1022.
- [85] M. Makri, C.G. Vayenas, S. Bebelis, K.H. Besocke, and C. Cavalca, *Surf. Sci.* **369** (1996) 351–359.
- [86] S. Ladas, S. Bebelis, and C.G. Vayenas, *Surf. Sci.* **251/252** (1991) 1062–1068.
- [87] Y. Jiang, I.V. Yentekakis, and C.G. Vayenas, *J. Catal.* **148** (1994) 240–251.
- [88] D. Kek, M. Mogensen, and S. Pejovnik, *J. Electrochem. Soc.* **148** (8), (2001) A878–A886.
- [89] M. Boudart, and G. Djéga-Mariadassou, *Kinetics of Heterogeneous Catalytic Reactions*, Princeton Univ. Press, Princeton, NJ (1984).
- [90] L.L. Hegedus, R. Aris, A.T. Bell, M. Boudart, N.Y. Chen, B.C. Gates, W.O. Haag, G.A. Somorjai, and J. Wei, *Cata-*

- lyst design: Progress and Perspectives, John Wiley & sons, New York (1987).
- [91] C.N. Satterfield, *Heterogeneous Catalysis in Industrial Practice*, McGraw-Hill, Inc. (1991).
- [92] R.J. Farrauto, and C.H. Bartholomew, *Fundamentals of industrial catalytic processes*, Chapman & Hall, London (1997).
- [93] G. Ertl, H. Knötzinger, and J. Weitcamp, *Handbook of Catalysis*, VCH Publishers, Weinheim (1997).
- [94] S.J. Tauster, S.C. Fung, and R.L. Garten, *JACS* **100** (1978) 170-175.
- [95] G.L. Haller, and D.E. Resasco, *Adv. Catal.* **36** (1989) 173-235.
- [96] E.C. Akubuiro, and X.E. Verykios, *J. Catal.* **113** (1988) 106-119.
- [97] M. Haruta, A. Ueda, S. Tsubota, and R.M.T. Sanchez, *Catalysis Today* **29** (1996) 443-447.
- [98] Y. Iizuka, H. Fujiki, N. Yamauchi, T. Chijiwa, S. Arai, S. Tsubota, and M. Haruta, *Catalysis Today* **36** (1997) 115-123.
- [99] S. Tsubota, D.A.H. Cunningham, Y. Bando, and M. Haruta, Preparation of nanometer gold strongly interacted with TiO<sub>2</sub> and the structure sensitivity in low-temperature oxidation of CO, in *Preparation of catalysts VI*, G. Ponchelet, ed. (1995), pp. 227-235.
- [100] Z. Hong, K.B. Fogash, and J.A. Dumesic, *Catalysis Today* **51** (1999) 269-288.
- [101] Y.D. Kim, A.P. Seitsonen, and H. Over, *Surf. Sci.* **465** (2000) 1-8.
- [102] D.G. Barton, M. Shtein, R.D. Wilson, S.L. Soled, and E. Iglesia, *J. Phys. Chem.* **103** (4), (1999) 630-640.
- [103] G. Meitzner, and E. Iglesia, *Catalysis Today* **53** (1999) 433-441.
- [104] B.L. Mojet, J.T. Miller, D.E. Ramaker, and D.C. Koningsberger, *J. Catal.* **186** (1999) 373-386.
- [105] S. Tagliaferri, R.A. Koeppel, and A. Baiker, *Appl. Catal. B* **15** (1998) 159-177.
- [106] A.Y. Stakheev, and L.M. Kustov, *Appl. Catal. A* **188** (1999) 3-35.
- [107] A. Cimino, D. Gazzoli, and M. Valigi, *Journal of Electron Spectroscopy and Related Phenomena* **104** (1999) 1-29.
- [108] S. Rossignol, C. Micheaud-Especel, and D. Duprez, *Stud. Surf. Sci. Catal.* **130** (2000) 3327-3332.
- [109] R.M. Ferrizz, T. Egami, and J.M. Vohs, *Surf. Sci.* **465** (2000) 127-137.
- [110] J. Kuriacose, *Industrial Journal of Chemistry* **5** (1957) 646.
- [111] S.J. Teichner *New Aspects of Spillover Effect in Catalysis for Development of Highly Active Catalysts in Third International Conference on Spillover*, (1993) Amsterdam, Elsevier, p. 27.
- [112] W.C. Conner, G.M. Pajonk, and S.J. Teichner, *Adv. Catal.* **34** (1986) 1-79.
- [113] B. Delmon, and H. Matralis, The remote control mechanism, general phenomena, possible consequences concerning unsteady state processes, unsteady state processes in catalysis, Y.S. Matros, ed. USF, Utrecht, The Netherlands (1991), p. 25.
- [114] T. Rebitzki, B. Delmon, and J.H. Block, *AIChE Journal* **41** (1995) 1543-1549.
- [115] B. Delmon, and G.F. Froment, *Catal. Rev.-Sci. Eng* **38** (1) (1996) 69-100.
- [116] H. Reiss, *J. Phys. Chem.* **89** (1985) 3783-3791.
- [117] P.M. Gundry, and F.C. Tompkins, in *Experimental Methods in Catalyst Research*, R.B. Anderson, ed. Academic Press, New York (1968), pp. 100-168.
- [118] J. Hölzl, and F.K. Schulte, *Work Function of Metals*, in *Solid Surface Physics*, Springer-Verlag, Berlin (1979), pp. 1-150.
- [119] S. Trasatti, *The Work Function in Electrochemistry*, in *Advances in Electrochemistry and Electrochemical Engineering*, H. Gerisher, and C.W. Tobias, eds., Journal Wiley and Sons (1977).
- [120] H.L. Skriver, and N.M. Rosengaard, *Physical Review B* **45** (16) (1992) 9410-9412.
- [121] C.G. Vayenas, S. Brosda, and C. Pliangos, *J. Catal.* **203** (2001) 329-350.
- [122] C.G. Vayenas, and S. Brosda, *Stud. Surf. Sci. Catal.* **138** (2001) 197-204.
- [123] S. Surnev, and M. Kiskinova, *Appl. Phys.* **46** (1988) 323-329.
- [124] G. Rangelov, and L. Surnev, *Surf. Sci.* **185** (1987) 457-468.
- [125] M. Kiskinova, *Surf. Sci.* **182** (1987) 150-160.
- [126] M. Kiskinova, and M. Tikhov, *Surf. Sci.* **194** (1988) 379-396.
- [127] G. Pacchioni, F. Illas, S. Neophytides, and C.G. Vayenas, *J. Phys. Chem.* **100** (1996) 16653-16661.
- [128] G. Pacchioni, J.R. Lomas, and F. Illas, *Molecular Catalysis A: Chemical* **119** (1997) 263-273.
- [129] D. Tsiplakides, and C.G. Vayenas, *J. Electrochem. Soc.* **148** (5), (2001) E189-E202.
- [130] C. Cavalca, G. Larsen, C.G. Vayenas, and G. Haller, *J. Phys. Chem.* **97** (1993) 6115-6119.
- [131] C.G. Vayenas, *J. Electroanal. Chem.* **486** (2000) 85-90.
- [132] A. Frumkin, and B. Damaskin, *J. Electroanal. Chem.* **79** (1977) 259-266.
- [133] S. Brosda, and C.G. Vayenas, *J. Catal.*, submitted (2001).
- [134] C.G. Vayenas, R.M. Lambert, S. Ladas, S. Bebelis, S. Neophytides, M.S. Tikhov, N.C. Filkin, M. Makri, D. Tsiplakides, C. Cavalca, and K. Besocke, *Stud. Surf. Sci. Catal.* **112** (1997) 39-47.
- [135] J. Nicole, D. Tsiplakides, C. Pliangos, X.E. Verykios, C. Comninellis, and C.G. Vayenas, *J. Catal.* **204** (2001) 23-34.
- [136] J. Nicole, and C. Comninellis, *J. Appl. Electrochem.* **28**, (1998) 223-226.
- [137] J. Nicole, PhD Thesis, EPFL (1999).
- [138] C. Pliangos, PhD Thesis, Department of Chemical Engineering, University of Patras (1997).
- [139] C.G. Vayenas, and G. Pitselis, *I&EC Research* **40** (20) (2001) 4209-4215.
- [140] C. Pliangos, I.V. Yentekakis, V.G. Papadakis, C.G. Vayenas, and X.E. Verykios, *Appl. Catal. B* **14** (1997) 161-173.
- [141] C.T. Campbell, *J. Phys. Chem.* **89** (26), (1985) 5789-5795.
- [142] C.T. Campbell, and B.E. Koel, *Surf. Sci.* **183** (1987) 100-112.
- [143] I.V. Yentekakis, R.M. Lambert, M.S. Tikhov, M. Konsolakis, and V. Kioussis, *J. Catal.* **176** (1998) 82-92.
- [144] F.A. Alexandrou, V.G. Papadakis, X.E. Verykios, and C.G. Vayenas *The promotional effect of Na on the NO reduction by CO on supported Pt, Pd and Rh catalysts in Proc. 4th Intl. Congress on Catalysis and Automotive Pollution Control* **2**, (1997), pp. 1-16.
- [145] D. Tsiplakides, S. Neophytides, and C.G. Vayenas, *Ionics* **3** (1997) 201-208.
- [146] D. Tsiplakides, S. Neophytides, and C.G. Vayenas, *Solid State Ionics* **136-137** (2000) 839-847.
- [147] D. Tsiplakides, S. Neophytides, and C.G. Vayenas, *Ionics* **7** (3) (2001) 203-209.
- [148] A. Frantzis, PhD Thesis, University of Patras (2002).

## IZVOD

## ZAKONI I MODELOVANJE FENOMENA INICIJACIJE, ELEKTROHEMIJSKE INICIJACIJE I INTERAKCIJE METAL-NOSAČ KATALIZATORA

(Pregledni rad)

Costas G. Vayenas, Costas Plinagos, Susanne Brosda, Dimitrios Tsiplakides  
Katedra za hemijsko inženjerstvo, Univerzitet u Patrasu, Patras, Grčka

U posljednje tri godine bilo je interesantnog razvoja teorije i otkrića u oblasti katalize i elektrohemijskih procesa koji uključuju katalizator kao čvrstu fazu. Prvo, pokazano je da postoji funkcionalna identičnost između fenomena iniciranja, elektrohemijskog iniciranja (NEMCA-efekt) i interakcije između metal-nosač čvrstog katalizatora. Drugo, definisan je koncept apsolutnog potencijala kod elektrohemijskih procesa koji uključuju čvrst katalizator, a koji uključuje vezu između operativnih funkcija nosača katalizatora i istih u odnosu na interakciju između metala i nosača katalizatora. Treće, vrlo stroga pravila su uspostavljena između inicijacije, elektrohemijske inicijacije i interakcije metal-nosač katalizatora. Ova pravila (zakoni) omogućavaju da se predvidi tip promotora ili nosača koji su neophodni za ostvarivanje neke katalitičke reakcije na bazi poznavanja kinetike iste reakcije bez prisustva katalizatora. Četvrto, detaljno je razvijeno proširenje Langmuir-Hinshelwood-ovog mehanizma koje eksplicitno uzima u obzir interakciju adsorbovanih molekula i dvostrukog filma stvorenog na međufaznoj površini između katalizatora (čvrste) i gasovite faze. Pokazano je da je novi tip kinetike katalitičkog procesa u potpunosti saglasan sa eksperimentima.

U radu se analiziraju ovi koncepti sa ciljem da se najnovija otkrića u oblasti iniciranja, elektrohemijskog iniciranja reakcije i interakcije metal-nosač katalizatora definišu kao katalitički proces u prisustvu elektrohemijskog dvostrukog filma.

Ključne reči: Kataliza • Elektro-kataliza • NEMCA • Interakcija metal-nosač •  
Key words: Catalysis • Solid state electrochemistry • NEMCA • metal-support interactions •

**Costantino (Costas) G. Vayenas**

He was born in Athens in 1950 and got his Diploma in Chemical Engineering from the National Technical University of Athens in 1973 and his PhD in Physical Chemistry from the University of Rochester in 1976. He then taught as Assistant Professor at Yale (1976-77) and as Assistant and Associate Professor of MIT (1977-81) before joining the University of Patras as Professor in 1981. His research interests are in electrochemistry, catalysis, electrochemical promotion of catalysis (an area discovered by his group), chemical and electrochemical reaction engineering and physical chemistry of reinforced concrete. He has authored some 180 scientific papers and several books including the "Electrochemical activation of Catalysis" (Kluwer/Plenum Press, 2002). He is also coeditor of the book "Catalysis and Electrocatalysis at nanoparticle surfaces" (Marcel-Dekker, 2002). He is editor of Ionics, guest editor of Solid State Ionics and a member of the International Editorial board of Chemical Industry H. (Belgrade). He recently succeeded Professor J.O'M. Bockris as co-editor of Modern Aspects of Electrochemistry.

Costas Vayenas has received the Dreyfus Teacher-Scholar Award in 1982, the Academy of Athens Award in Chemistry in 1992, the Wason Medal of the American Concrete Institute in 1992 and the Outstanding Achievement Award of the Electrochemical Society (High Temperature Materials Division) in 1996. He is currently vice-rector of the University of Patras and vice-president of the National Research Council of Greece.

**Costas Plinagos**

He was born in Athens, Greece in 1966. He received PhD from the department of Chemical Engineering, University of Patras (Greece), in 1995. His recent research interests are focused in the areas of nanoparticles technology (particularly catalysts and ceramic ionic conductors) for chemical processes and fuel cells, chemical kinetics and heterogeneous catalysis, automotive exhaust catalytic converters and chemistry of air pollution control, as well as in electrochemistry and electrocatalysis.

C. Plinagos is member of several scientific societies such as International Electrochemical Society, Panhellenic Catalytic Society and Technical Chamber of Greece. He is currently employed in University of Patras as associate researcher in the Department of Chemical Engineering (Laboratory of Chemical and Electrochemical Processes, and as lecturer in the Department of Material Science.

**Susanne Brosda**

She was born in Merseburg, Germany in 1965 and got her Diploma in Chemistry and PhD in Physical Chemistry at the University of Greifswald. She was a visiting researcher at the University of Tübingen, in the group of the late Professor W. Göpel, and a research engineer at Heraeus Sensor Nite N.V. in Belgium before joining the University of Patras in 1998 as a TMR postdoctoral fellow. Her research interests are in solid state sensors and in electrochemical promotion of catalysis.

**Dimitrios Tsiplakides**

Born in Thessaloniki, Greece in 1973. Received his PhD degree from the Department of Chemical Engineering, University of Patras in 2001 where he is currently a postdoctoral research associate. His current research interests are in heterogeneous catalysis, chemical kinetics and reaction engineering, surface science, electrochemistry, electrocatalysis and fuel cells. He has coauthored the "Electrochemical Activation of Catalysis", Kluwer/Plenum Press 2002.

